Università degli Studi di Cagliari

Ph.D. DEGREE

Molecular and Translational Medicine

Cycle XXXIV

Comprehensive analysis of mRNA-miRNA network in preneoplastic hepatocytes undergoing regression following treatment with thyroid hormone.

Department of Biomedical Sciences

Unit of Oncology and Molecular Pathology

Scientific Disciplinary Code: Med/04

PhD student Rajesh Pal

Supervisor Prof. Andrea Perra

Final exam 2020/2021

Thesis defence: April 2022 Session

TABLE OF CONTENTS

1. ABBREVIATIONS

2-AAF	2-acetylaminofluorene
ANOVA	Analysis of variance
BH	Benjamini-Hochberg
DE	Differentially expressed
DEN	Diethylnitrosamine
Dio1	Deiodinase 1
FC	Fold change
FDR	False discovery rate
FXR	Farnesoid X receptor
G6PD	Glucose-6-phosphate dehydrogenase
GAPDH	Glyceraldehyde 3-phosphatase dehydrogenase
GFF/GTF	General Transfer Format
GST-P	Placental form of glutathione-S-transferase
HBV	Hepatitis B virus
HCC	Hepatocellular carcinoma
HCV	Hepatitis C virus
IPA	Ingenuity Pathway Analysis
IPA	Ingenuity Pathways Analysis
Keap1	Kelch Like ECH Associated Protein 1
Krt-19	Cytokeratin-19
miRNA/miR	MicroRNA
miRNA-seq	microRNA sequencing
mRNA	Messenger RNA
NASH	Non-alcoholic steatohepatitis
NGS	Next generation sequencing
Nqo1	NAD(P)H Quinone Dehydrogenase 1

Nrf2	Nuclear factor erythroid 2–related factor 2
NSCLC	Non-small cell lung cancer
OXPHOS	Oxidative phosphorylation
PCA	Principal Component Analysis
PCA	Principal component analysis
PH	Partial hepatectomy
PPP	Pentose phosphate pathway
QC	Quality control
qRT-PCR	Quantitative Reverse Transcription PCR
RAS	Rat sarcoma virus
R-H	Resistant-Hepatocyte
RIDE	RNA Differential Expression
RIN	RNA integrity number
RNA-seq	RNA sequencing
ROS	Reactive oxygen species
RXR	Retinoid X receptor
SD	Standard Deviation
SDH	Succinate Dehydrogenase Complex
SRA	Sequence Read Archive
SRIDE	small RNA Differential Expression
TH	Thyroid hormone
THR	Thyroid responsive elements
TSH	Thyroid stimulating hormone
UMI	Unique molecular Identifier
UTR	Untranslated region

2. ABSTRACT

Background: Hepatocellular carcinoma (HCC) is the third leading cause of cancer-related deaths worldwide. Despite the approval of new molecular targeted therapies, benefits from current therapies remain unsatisfactory. Thus, it is mandatory to find new and effective therapeutic treatment strategies to treat HCC. Recent studies revealed a status of severe local hypothyroidism in rat hepatic preneoplastic lesions, and in human HCCs, suggesting that this condition may represent a favorable event for HCC development. Accordingly, a short treatment with thyroid hormone (T3) caused the regression of pre-neoplastic lesions in a rat model of hepatocarcinogenesis.

Thyroid hormones (THs) inhibit HCC through different mechanisms. To investigate whether microRNAs (miRs) play a role in the antitumorigenic effect of THs, by Next Generation Sequencing (NGS) we performed a comprehensive comparative miRNomic and transcriptomic analysis of hepatic preneoplastic lesions of rats subjected to the Resistant-Hepatocyte (RH) protocol and then exposed or not to a four-day treatment with triiodothyronine (T3). The most deregulated miRs were also analysed in HCCs generated by the same protocol, with or without T3.

Analysis of the transcriptomics data can be tricky, and often requires substantial expertise in bioinformatics. Prior to the final analysis, the raw data needs to be processed through number of steps, thus resulting in a gene or miRNA expression quantification. Bioinformatic workflows are generally employed to automate these steps. A number of workflows are available to help the researchers preprocess their data. However, many existing workflows have their own approach towards the analysis, or they are limited to specific studies. Here, we have implemented two automated, scalable, and reproducible Snakemake based pipelines called RIDE and SRIDE for performing transcriptome and microRNA analysis respectively.

Result: Pathway analysis in preneoplastic nodules showed that Oxidative Phosphorylation and NRF2-mediated Oxidative Stress Response were the most deregulated pathways. These pathways were resulted to be reversed in preneoplastic nodules exposed to T3. Gene expression analysis showed that T3 also inhibited proline biosynthesis, which was up-regulated in preneoplastic lesions. With regard to microRNA, most downregulated miRNA in preneoplastic lesions have already been described to act as oncosuppressors, whereas, some of the differentially up-regulated

miRNAs have been shown to contribute substantially in carcinogenesis process. miRNA's down-regulated in preneoplastic nodules following T3 treatment targeted Thyroid hormone receptor-β (THRβ), deiodinase, and oxidative phosphorylation pathways, while on the contrary, most upregulated miRNAs were those of targeting Nrf2 Oxidative Pathway, Glycolysis, Pentose Phosphate Pathway and Proline biosynthesis – all involved in metabolic reprogramming. Notably, while T3 exerted similar effects on gene expression in both preneoplastic nodules and HCCs, no change in the expression of these miRNAs regulated in preneoplastic lesions was found at the late stages.

This study investigated the miRNA-mRNA networks elicited by T3 treatment in liver preneoplastic lesions. The identification of several miRNAs, so far never associated to T3, may improve our understanding of the key regulator events underlying the early stages of HCC development and help to design therapeutic strategies.

3.INTRODUCTION

3.1. Hepatocellular Carcinoma

Primary liver cancer is the sixth most diagnosed cancer and is the third largest contributor to cancer mortality. Approximately, 906,000 new cases and 830,000 deaths were registered in the year 2020(Fig. 1). Hepatocellular carcinoma (HCC) is the most common form of liver cancer and accounts for ~90% of cases (1). Highest incidence and mortality rates are commonly observed in East Asia (China, Japan, Mongolia, North Korea, South Korea, and Taiwan) and Africa. Intermediate incidence rates are reported in countries of the Central Europe, while for Northern Europe, Middle East, Oceania and America the lowest incidence rates are registered. (2,3)

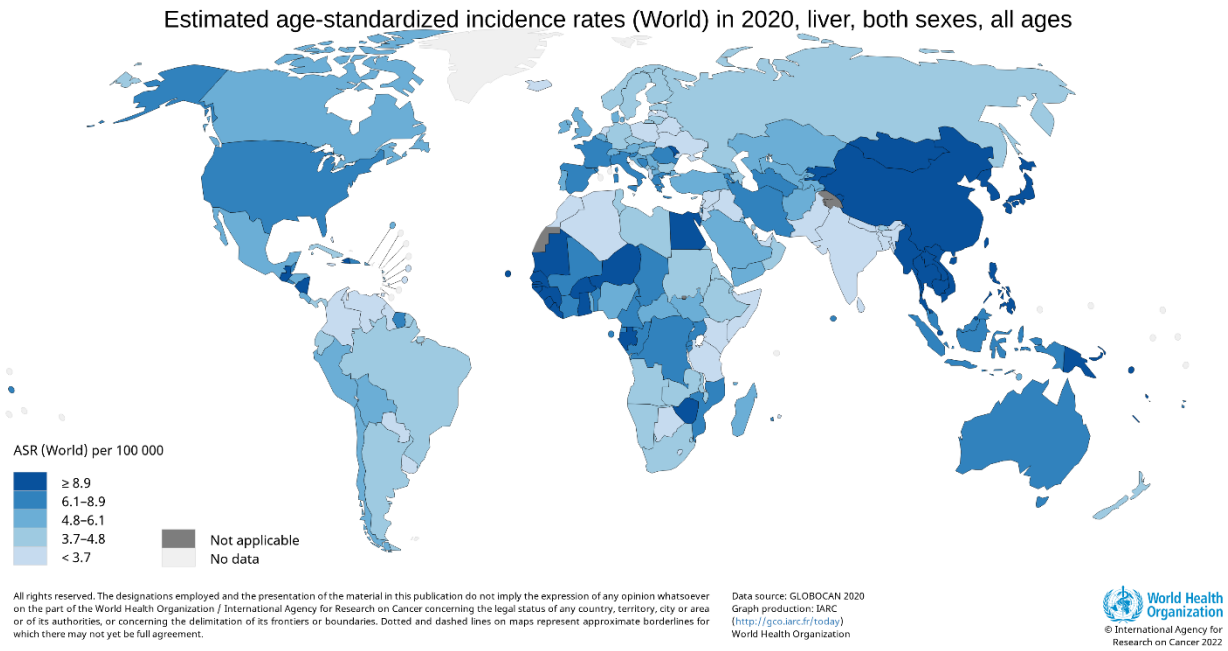

Fig. 1: Primary liver cancer incidence rates throughout the world. (Data source: Globocan 2020).

3.2. Risk Factors

The global incidence of HCC varies due to the variable prevalence of associated etiologies. The known risk factors for HCC are toxic (alcohol and aflatoxins), viral (chronic hepatitis B and hepatitis C), immune-related (primary biliary cirrhosis and autoimmune hepatitis) and metabolic (diabetes and non-alcoholic fatty liver disease, hereditary haemochromatosis) (4,5)

Hepatitis B virus infection (HBV)

Globally about 296 million people are living with chronic hepatitis B infection (6). HBV is a hepatotropic DNA virus that integrates its DNA in to the host genome, thus inducing both host chromosomal instability and insertional mutagenesis of HCC related genes (7). Among the individuals with chronic HBV infection, 15 to 40% progress to cirrhosis, thus leading to liver failure and liver cancer(8). HBV infection is passed down from person to person through blood, semen or other body fluids. Over the years, HBV vaccination programmes has dramatically reduced HCC incidence in some parts of Asia, however effective vaccination programmes are yet to be implemented (9,10).

Hepatitis C virus infection (HCV)

Hepatitis C virus (HCV), is a hepatotropic RNA virus which causes chronic liver disease. About 58 million people have chronic HCV worldwide, with about 1.5 million new incidences being reported every year (11). Unlike HBV, HCV does not integrate in to the host genome, therefore the risk of HCC is primarily limited to those who develop cirrhosis or chronic liver damage(12). Since it's a bloodborne virus, major risk factors include exposure to blood from unsafe injection practices, unsafe health care, injection use and unscreened blood transfusion. Currently, there is not effective vaccine against hepatitis C. However, direct-acting antiviral (DAA) therapy can cure 95% of people with HCV infection (11,13)

Non-Alcoholic Fatty liver Disease (NAFLD)

Non-alcoholic fatty liver disease (NAFLD) affects a third of the world's population. Globally, 25% of the general population is thought to be suffering from NAFLD, with the highest incidence rate in South America and Middle East (30.45% and 31.79% respectively) and lowest in Africa (13.48%) (14). Primary causes of NAFLD are obesity and diabetes. Not only they contribute to

the development of the disease, but are also independent risk factors for HCC (15,16). Other risk factors include genetic predisposition, which explains the variability in NAFLD phenotype and risk of progression. NAFLD can progress to non-alcoholic steatohepatitis (NASH), fibrosis, cirrhosis and to HCC. NAFLD associated HCC can be prevented by adopting healthy lifestyle, use of anti-fibrotic therapies and use of pharmacological therapy, such as statins and metformin (17,18).

Alcohol

Excessive alcohol intake results in fatty liver, acute/chronic hepatitis, cirrhosis and eventually leads to HCC(19). At present, there is a surge in the number of persons that have cirrhosis due to alcohol consumption or NASH. The incidence of alcohol induced liver carcinogenesis is highest in developed countries, especially in Europe and USA(20). In population-based study, the annual incidence of alcohol induced cirrhosis ranges from 1% to 2-3% in tertiary care referral centers and accounts for ~15-30% of HCC cases (21). Risk factor that initiates the alcohol-induced liver damage and the development of HCC include the amount of ethanol consumption, gender differences, coexistence of hepatitis virus, diabetes and obesity(22) .

Age, sex, and other factors

HCC has been associated with several sociodemographic characteristics, particularly in patients with cirrhosis. Aging is considered to be a strong risk factor, with the age specific incidence reported in individuals over 70 years of age (23). Additionally, the number of HCC cases has been predominantly seen in males, likely due to the differences in sex hormones and clustering of risk factors(1). Studies show that a higher incidence of HCC is reported among ethnic minorities or racial groups, particularly in Hispanics, when compared to white individuals. The high incidence rate in minorities might be partly due to the single nucleotide variation in PNPLA3 gene, which is linked to NASH associated HCC (24).

3.3. Therapeutic strategies for HCC

Over the years outcome of patients with HCC has substantially improved. Better outcomes can be attributed to earlier detection as a result of the wider implementation of surveillance programs, advances in effective treatments and better management of underlying liver disease (25). Treatment options largely depend on tumor stages and the expected benefits of major

interventions, following the Barcelona Clinic Liver Cancer (BCLC) staging system (26–28) (Fig 2). According to the guidelines, early-stage HCC patients are mostly preferred for transplantation, resection and local ablation, whereas patients at intermediate stages are preferred for locoregional treatments like transarterial chemoembolization (TACE) and those with advanced HCC (aHCC) receive systemic therapies (Fig. 2).

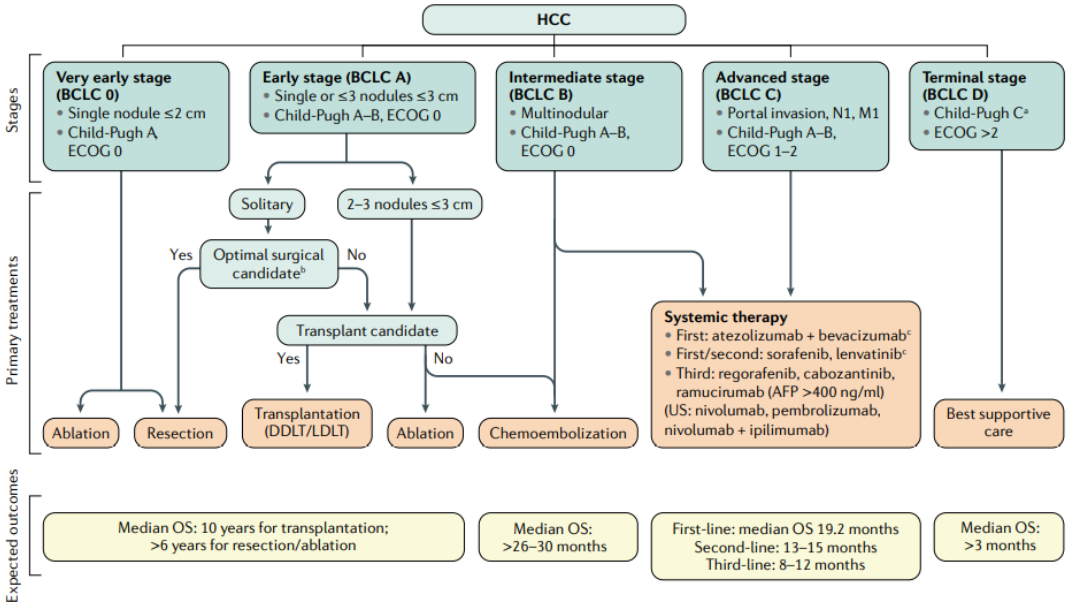

Fig. 2 Based on the disease extension and liver function, the Barcelona Clinic Liver Cancer (BCLC) staging system consists of 5 stages. Local curative treatments (ablation, resection or transplantation, depending on the presence of portal hypertension, number of nodules and liver function) are given to the asymptomatic patients with low tumor burden and good liver function (BCLC 0/A). Asymptomatic patients with multinodular disease and adequate liver function (BCLC B) should receive chemoembolization and patients with portal thrombosis or extrahepatic spread (BCLC C) should be treated with systemic therapies.(12)

The landmark success of Asia-Pacific and SHARP trial led to the approval of sorafenib, a multikinase inhibitor, as first-line targeted therapy for advanced HCC (26,29–31) . Over the past 10 years, sorafenib has been the standard care for patients with unresectable HCC. Recently, several other multikinase inhibitors were approved as first line agents, such as Lenvatinib, Donofenib etc. Each of the drug demonstrated superior OS (Overall Survival) outcomes compared to sorafenib (32).

Sorafenib displays limited anti-tumor activity and both adaptive resistance and intrinsic resistance represents crucial challenge in the management of patients receiving first line treatment of HCC (33). Treatment options for patients with advanced HCC have greatly improved with the introduction of tyrosine-kinase inhibitors (TKI) and recently immune checkpoint inhibitors (ICI) (Fig. 3)(34,35)

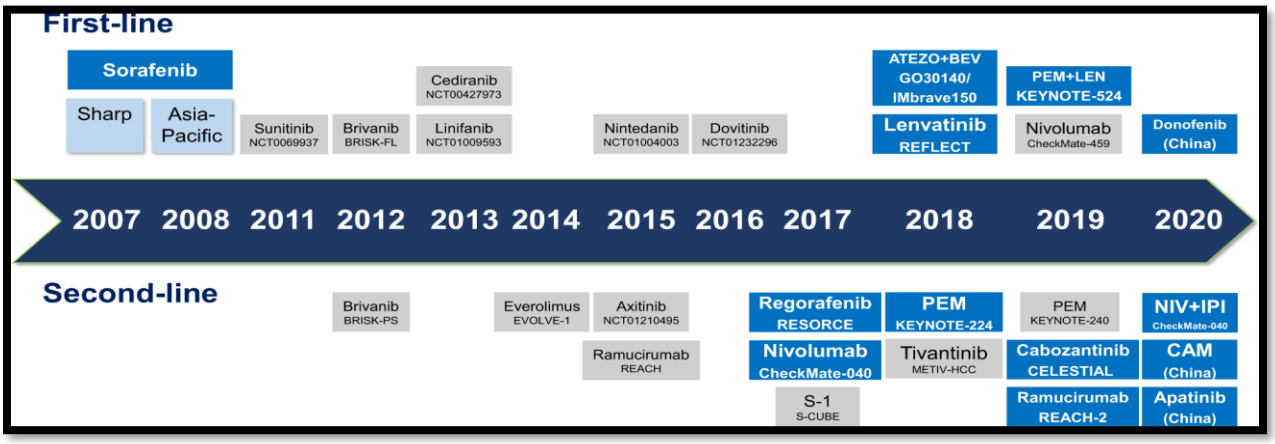

Fig. 3: Overview of the targeted agents approved for HCC. ATEZO (atezolizumab), BEV (bevacizumab), CAM (camrelizumab), LEN (lenvatinib), PEM (pembrolizumab), NIV (nivolumab), IPI (ipilimumab) (35)

Drug resistance in HCC still remains challenging due to random mutations in target receptors as well as downstream pathways. ICIs have been shown to be an evolving novel treatment option in certain advanced solid tumors and have been recently approved for inoperable, advanced, and metastatic HCC. Unfortunately, a large cohort of patients with HCC fail to respond to immunotherapy (36). Researchers have applied different therapeutic strategies combining ICIs with other agents. Many of the strategies have obtained positive results in early clinical trials and are currently being tested in phase III trials. (Table 1).

Drug	Targets	Stage and conditions	Phase	Primary endpoint(s)	ClinicalTrails.gov	Study start
Immunotherapy plus Anti-angiogenesis						
Atezolizumab plus Lenvatinib or Sorafenib	PD-L1 + VEGFRs, FGFRs, PDGFR a, RET, KIT and RAF	Advanced; Second-line	III	OS	NCT04770896	2021
SHR-1210 plus Apatinib	PD-1 + VEGFR-2	Advanced; First-line	III	OS/PFS	NCT03764293	2019
CS1003 plus Lenvatinib	PD-1 + VEGFRs. FGFRs, PDGFR a, RET and KIT	Advanced; First-line	III	OS/PFS	NCT04194775	2019
Durvalumab plus Bevacizumab	PD-L1 + VEGFA	High risk of recurrence; Second-line	III	RFS	NCT03847428	2019
Atezolizumab plus Bevacizumab	PD-L1+ VEGFA	Locally advanced or metastatic First-line	III	OS/PFS	NCT03434379	2018
Atezolizumab plus Cabozantinib	PD-L1 + VEGFR, MET, RET, KIT and AXL	Advanced; First-line	III	OS/PFS	NCT03755791	2018
Pembrolizumab plus Lenvatinib	PD-1 + VEGFRs, FGFRs, PDGFR a. RET and KIT	Advanced; First-line	III	OS/PFS	NCT03713593	2018
Nivolumab plus Sorafenib	PD-1 + VEGFRs, KIT, PDGFRs, and RAF	Locally Advanced or Metastatic; First-line	II	MTD/ORR	NCT03439891	2018
Avelumab plus Regorafenib	PD-L1 + VEGFR1-3, PDGFR-I3, FGFR1, KIT, RET and B-RAF	Advanced or metastatic	I/II	RP2D/ORR	NCT03475953	2018
Nivolumab plus Cabozantinib	PD-1 + VEGFR, MET, RET, KIT and AXL	Locally Advanced; Neoadjuvant	I	AEs	NCT03299946	2018
Nivolumab plus Bevacizumab	PD-1 + VEGFA	Advanced or Metastatic	I	AEs/MTD or RP2D	NCT03382886	2018
Durvalumab plus Cabozantinib	PD-L1 + VEGFR, MET, RET, KIT and AXL	Advanced; Second-line	I	MTD	NCT03539822	2018
Nivolumab plus Vorolanib	PD-1 + VEGFR, PDGFR	/	I	RP2D	NCT03511222	2018
PDR001 plus Sorafenib	PD-1 + VEGFRs, KIT, PDGFRs, and RAF	Advanced; First-line	I	AEs	NCT02988440	2017
Pembrolizumab plus Regorafenib	PD-1 + VEGFR1-3, PDGFR-I3, FGFR1, KIT, RET and B-RAF	Advanced; First-line	I	AEs/DLTs	NCT03347292	2018
Durvalumab plus Ramucirumab	PD-L1 + VEGFR2	Advanced or metastatic	I	DLTs	NCT02572687	2016

Inmunotherapy plus other agents						
IBI310 plus Sintilimab	CTLA-4 + PD-1	Advanced; First-line	III	OS/ORR	NCT04720716	2021
Nivolumab plus Ipilimumab	PD-1 + CTLA-4	Advanced; First-line	III	OS	NCT04039607	2019
Durvalumab plus Tremelimumab	PD-L1 + CTLA-4	Advanced; First-line	III	OS	NCT03298451	2017
TSR-042 plus TSR-022	PD-1 +TIM-3	Locally advanced or metastatic	II	ORR	NCT03680508	2018
Pembrolizumab plus Bavitcodmab	PD-1 + PS	Advanced; First-line	I/II	ORR	NCT03519997	2018
Nivolumab plus MS-986205	PD-1 +1DO1	Advanced; First-line	I/II	AEs/ORR	NCT03695250	2018
Pembrolizumab plus Epacadostat	PD-1 +1DO1	/	I/II	DLTs/ORR	NCT02178722	2014
Pembrolizumab plus INCAGN01876 plus Epacadostat	PD-1 + GITR+IDO1	Advanced	I/II	AEs/ORR	NCT03277352	2017
Nivolumab plus Galunisertib	PD-1 + TβR1	Advanced; Recurrent	I	MTD	NCT02423343	2015
Nivolumab plus Avadornide	PD-1 + 018N	Unresectable	I	DLT/AB/ORR	NCT02859324	2016
Pembrolizumab plus VSV-IFNβ -NIS	PD-1 + Oncolytic virus	Refractory	I	ORR/AEs	NCT03647163	2019
Durvalumab plus Guadecitabine	PD-L1 + DNMT	Advanced; Metastatic	I	AEs/ORR	NCT03257761	2018
Pembrolizumab plus XL1888	PD-1 + Hsp90	Advanced; Metastatic	I	RP2D	NCT03095781	2017
Pembrolizumab plus Vaccine	PD-1 + Modified Vaccinia Virus Ankara Vaccine Expressing p53	Unresectable; Second-line	I	Tolerability	NCT02432963	2015
PDR001 plus NIS793	PD-1 + TGF-β	Advanced	I	DLTs/PEs	NCT02947165	2017
Nivolumab plus SF1126	PD-1 + PI3K	Advanced	I	DLT	NCT03059147	2017

Other combination						
Apatinib plus Capecitabine	VEGFR-2 + DNA/RNA Synthesis	Advanced	II	TIP	NCT03114085	2017
Temsirolimus plus Sorafenib	mT0R+VEGFFts, KIT, PDGFRs, and RAF	Advanced; First-line	II	TTP	NCT01687673	2012
Trametinib plus Sorafenib	MEK 1/2 + VEGFRs, KIT, PDGFRs, and RAF	Advanced	I	MID	NCT02292173	2014
CVM-1118 plus Sorafenib	VM + VEGFRs, KIT, PDGFRs, and RAF	Advanced	II	ORR	NCT03582618	2018
mFOLFOX plus Sorafenib	DNA Synthesis+VEGFRs, KIT, PDGFRs, and RAF	/	II	TIP	NCF01775501	2013
Erlotinib plus Bevadzumab	EGFR+VEGFA	Advanced; Second-line	II	PFS (16 W)	NCT01180959	2011
TRC 105 plus Sorafenib	Endoglin+VEGFRs, 10T, PDGFRs, and RAF	/	I/II	MTD/ORR	NCT02560779	2016
Enzalutamide plus Sorafenib	AR + VEGFRs, 10T, PDGFRs, and RAF	Advanced; First-line	I/II	PFs	NCT02642913	2015
Napabucasin or Amcasertib plus Sorafenib	STAT3, cancer sternness kinase+VEGFRs, KIT, PDGFRs, and RAF	Advanced; First-line	I/II	RP2D/AB5JAA	NCT02279719	2014
ADI-PEG 20 plus FOLFOX	Arginine+DNA Synthesis	Advanced	I/II	ORR	NCT02102022	2014
FATE-NK1E0 plus Cetuximab or Trastuzumab	NK cell immunothempy+EGFR or EGFR2	EGFR1+ or HER2+; Advanced	I	DLT	NCT03319459	2018
Navitodax plus Sorafenib	13d-2 + VEGFRs, KIT, PDGFRs, and RAF	Relapsed or refractory	I	MTD/AS	NCT02143401	2014

Table 1: Abbreviations: PD-1 programmed cell death-1, VEGFR vascular endothelial growth factor receptor, VEGF vascular endothelial growth factor, PD-L1 programmed cell death ligand 1, FGFR fibroblast growth factor receptor, FGF fibroblast growth factor, PDGFR platelet derived growth factor receptor, CTLA-4 cytotoxic T lymphocyte–associated antigen-4, TIM-3 T-Cell immunoglobulin and mucin domain-containing molecule 3, PS phosphatidylserine, IDO1 indoleamine 2,3-Dioxygenase 1, GITR glucocorticoid-induced tumor necrosis factor receptor, TβRI transforming growth factor beta receptor 1, CRBN cereblon, DNMT DNA methyltransferase, Hsp90 heat shock protein 90, TGF-β transforming growth factor beta, PI3K phosphatidylinositol 3-kinase, mTOR mechanistic target of rapamycin kinase, VM vasculogenic mimicry, EGFR epidermal growth factor receptor, AR androgen receptor, STAT3 signal transducer and activator of transcription 3, OS overall survival, PFS progress free survival, MTD maximum tolerated dose, ORR objective response rate, RP2D recommended phase II dose, AEs adverse events, DLT dose limited toxicity, TTP time to progress, AA antitumor activity, RFS recurrence free survival

Benefits from present treatment options are still disappointing, as it extends the median life expectancy of patients by only few months. Thus, it is mandatory to find alternative treatment options. Several studies have reported aberrant THR expression and somatic mutations in human cancers, supporting the hypothesis that they might play a role in tumor development. Indeed, two independent case-control studies suggested that hypothyroidism represents a risk factor for human HCC (37,38) and a recent work showed that TRβ expression correlated with more progressed stages of non-alcoholic steatohepatitis (NASH), a well-known pro-tumorigenic condition (39). Experimental and clinical studies revealed a status of severe local hypothyroidism in rat hepatic preneoplastic lesions, and in human HCCs (40–42), suggesting that this condition may represent a favorable event for HCC development. Accordingly, T3 exogenous administration not only inhibited liver tumor formation but also induced regression of HCCs in vivo (43). The effect of T3 has been attributed to several mechanisms, including its ability to induce mitophagy, differentiation and metabolic reprogramming of pre- and neoplastic cells (43–45). In particular, it was shown that T3 can induce a switch of preneoplastic hepatocyte gene expression profile towards the one of fully differentiated cells (43).

3.4. Thyroid hormones (THs) and Thyroid Hormone Receptors (THRs) in HCC

Thyroid hormones, 3,5,3',5'-tetraiodo-L-thyronine (T4) and 3,5,3'-triiodo-L-thyronine (T3) are secreted by the follicular cells of the thyroid gland under control of the hypothalamic-pituitary axis. THs influence a variety of physiological processes, such as development, metabolism, cell growth and differentiation. The regulation of thyroid hormone begins at the hypothalamus. The hypothalamus releases Thyrotropin Releasing Hormone (TRH) that stimulates the pituitary gland to secrete the Thyroid Stimulating Hormone (TSH). TSH, in turn, stimulates the thyroid gland to release T3 and T4 and all this process is under control of a negative feedback loop (46). T4 constitutes more than 80% of the secreted hormone in the blood stream. Once transported across the cell membrane of responsive cells by specific monocarboxylate anion transporters such as MCT8 and MCT10, T4 is converted in to T3 that represent the physiological active form of T4. This conversion takes place in peripheral organs, mainly liver and kidney, and is carried out by the selenoenzymes iodothyronine deiodinase I and II (Dio1 and Dio2).

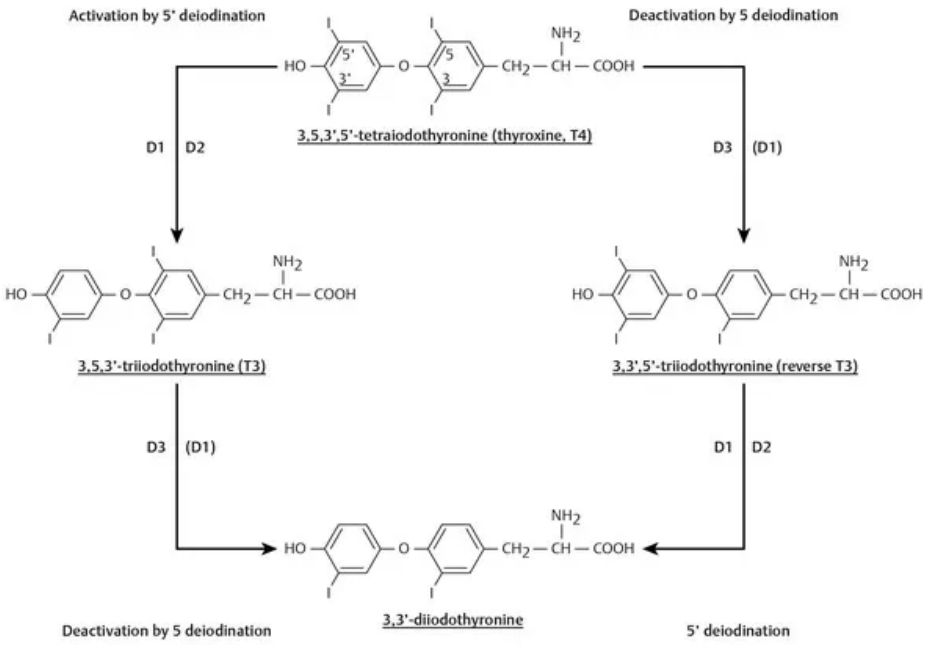

Fig. 4 Mechanisms of activation and inactivation of thyroid hormones. This is accomplished by the selenodeiodinases type 1 (D1) and type 2 (D2). Deiodination at the 5 position on the inner ring is accomplished by type 3 (D3) and D1 (47)

Dio1 is mainly expressed in kidney and liver, while Dio2 is expressed in pituitary gland, central nervous system, brown adipose tissue, uterus and placenta. Dio1 and Dio2 catalyze the outer ring 5'-deiodination that can be viewed as the first step in the activation of the thyroid hormone T4. Conversely, type III deiodinase is responsible for thyroid hormone inactivation converting T4 in reverse T3 (r T3) and both T3 and r T3 in the inactive form 3,3'-diiodothyronine (T2). T2 is sulfo- and glucuronide-conjugated before excretion the bile (46). TH could be re-uptaken through an enterohepatic circulation in which the intestinal flora deconjugates some of these compounds (Fig. 4)

Although it has been proposed that rapid non-genomic mechanisms initiated at the cell membrane could be involved in mediating some actions of thyroid hormones (48) most of the effects of THs on cellular proliferation and differentiation are driven by the thyroid hormone nuclear receptors (THRs) THRα and THRβ (49,50). THRs belong to the steroid/thyroid superfamily of nuclear hormone receptors which act as modulators of gene expression through

their ability to recognize specific DNA sequences. THRs are encoded by two genes THRα (NR1A1) and THRβ (NR1A2) localized in human chromosomal regions 17q11.2 and 3p24.3, and rat chromosomal regions 10q3 and 15p16, respectively. The expression of THRs isoforms is tissue dependent and developmentally regulated. THRα1 is constitutively expressed at embryonic development, and THRβ is expressed toward the later stage of development (51). THRα1 and THRα2 are expressed at the highest levels in the brain; at lower levels in the kidneys, skeletal muscle, lungs, heart, testes, and liver. THRβ1 is expressed predominantly in the kidneys, liver, brain, heart, and thyroid. THRβ2 is mainly expressed in the brain, retina, and inner ears (52). Liver, where THRβ represents the most abundant isoform (53,54), is an important target organ of THs and growing evidence implicates THs and THRs in HCC development.

3.5. THRs alterations in HCC

Previous studies have published conflicting results regarding the activating mutations in THR genes, thus suggesting THR mutations might play an oncogenic role in HCC development. However, recent exome sequencing study from TCGA-LIHC data reported no mutation in TRα, whereas only 1 (0.3%) mutation for THRβ gene, further validating that THR mutations are virtually absent in human HCC. Furthermore, no THR mutation have been reported in experimentally induced HCCs which aimed at detecting THRs mutation in chemically induced rat HCC(41).

Other than mutations, methylation profile of the THR could play a role in the carcinogenic process. Frequent hypermethylation of the TRβ promoter region has been reported in several human cancers (55–57). Nevertheless, methylation status of the THR promoter has not been reported in any of the independent or human HCC consortium studies.

Different studies have shown the effect of miRNA in TH signaling. While there is little or no evidence regarding miRNAs regulating the TH transporters, strong evidence suggests the regulation of deiodinases by miRNAs. miR-224 and miR-383 have been shown to downregulate Dio1 expression in renal cancer, while miR-214 and miR-21 have been shown to target Dio3 mRNA in mouse heart and hedgehog pathway-driven skin tumorigenesis respectively (58–62). Control of THRs expression levels by direct interaction of miRNA has also been described (Fig. 5). Although there is no evidence of TRα regulation by miRNAs yet, several miRNAs have been

shown to influence TRβ expression. High levels of miR-21, -146a, -181a and -221, all predicted to target TRβ, were found in papillary thyroid cancer (PTC) patients, in association with low levels of TRβ transcripts (63); moreover, TRβ expression in human clear cell renal carcinomas (ccRCC) was inversely correlated with the levels of miR-204 (64). Similarly, miR-155 and miR-425 have been shown to decrease TRβ expression in ccRCC.(63) miR-27a has been shown to regulate beta cardiac myosin heavy chain gene expression by targeting TRβ in neonatal rat ventricular myocytes (65). However, although a number of studies showed that miRNAs may be involved in repressing TRβ expression (63–66), which are the miRs targeted by THRs and what is their role in normal and genetically-altered hepatocytes remain elusive.

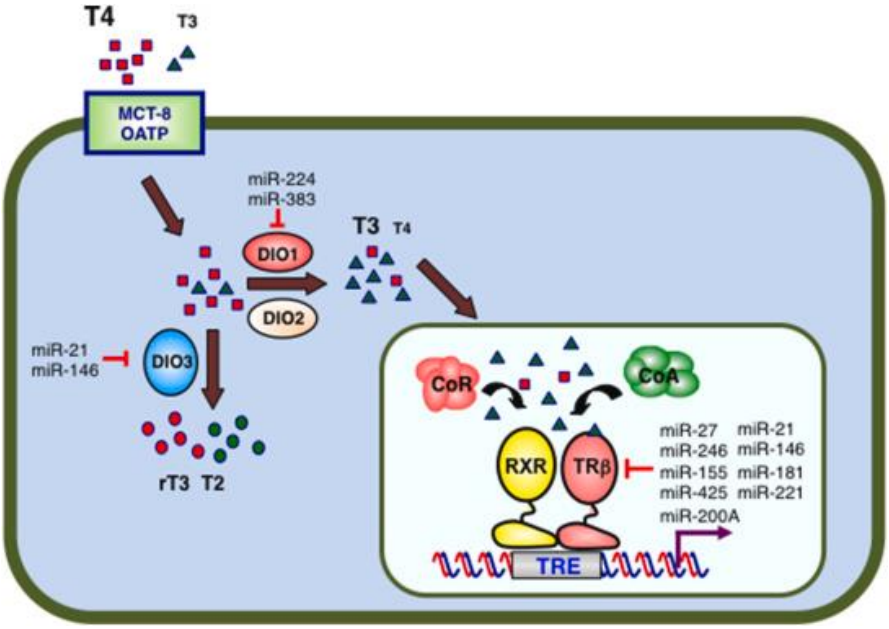

Fig. 5. The mRNAs of DIO1, DIO3, and TRβ are targets of the indicated miRNAs**.** The thyroid hormones (T4,T3,T2), transporter proteins (MCT8 or OATPs), Deiodinases 1,2 and 3 (DIO1,2,3), retinoid X receptor (RXR), thyroid hormone response elements (TREs), corepressor (CoR) and coactivator (CoA) complexes (67).

3.6. MiRNA biogenesis

MicroRNA's are a class of small non coding RNAs that play important roles in the regulation of gene expression and protein translation. Since their discovery by Ambros and colleagues, microRNA's have been identified as key regulators of complex biological processes such as development, differentiation, growth, apoptosis and metabolism(68–70). miRNAs have also been associated to many human diseases and are currently being pursued as clinical diagnostics and as therapeutic targets (71).

miRNA biogenesis is a multistep process, and it involves specific cellular machinery. Inside the nucleus, it begins with the transcription of the primary transcript by RNA polymerase II in to primary miRNA (pri-miRNAs) (72,73). Pri-miRNAs, which are the double stranded hairpin structures are cleaved to produce precursor miRNA (pre-miRNA) through microprocessor complex, which comprises of Drosha and DiGeorge Syndrome Critical Region8 (DGCR8) (74–77). The ~70 nucleotide pre-miRNA is exported in to the cytoplasm via Exportin5/RanGTP dependent manner and further cleaved to produce the ~20 nucleotide mature miRNA duplex (78–80). The cleavage process is mediated by Dicer. Finally, one of the two strands is loaded in to the Argonaute (AGO) family of proteins to form miRISC (miRNA-induced silencing complex) complex. miRNAs in the miRISC complex recognize the target mRNA and direct it for degradation and/or translation repression along with other RNA-binding proteins (Fig. 6) (81).

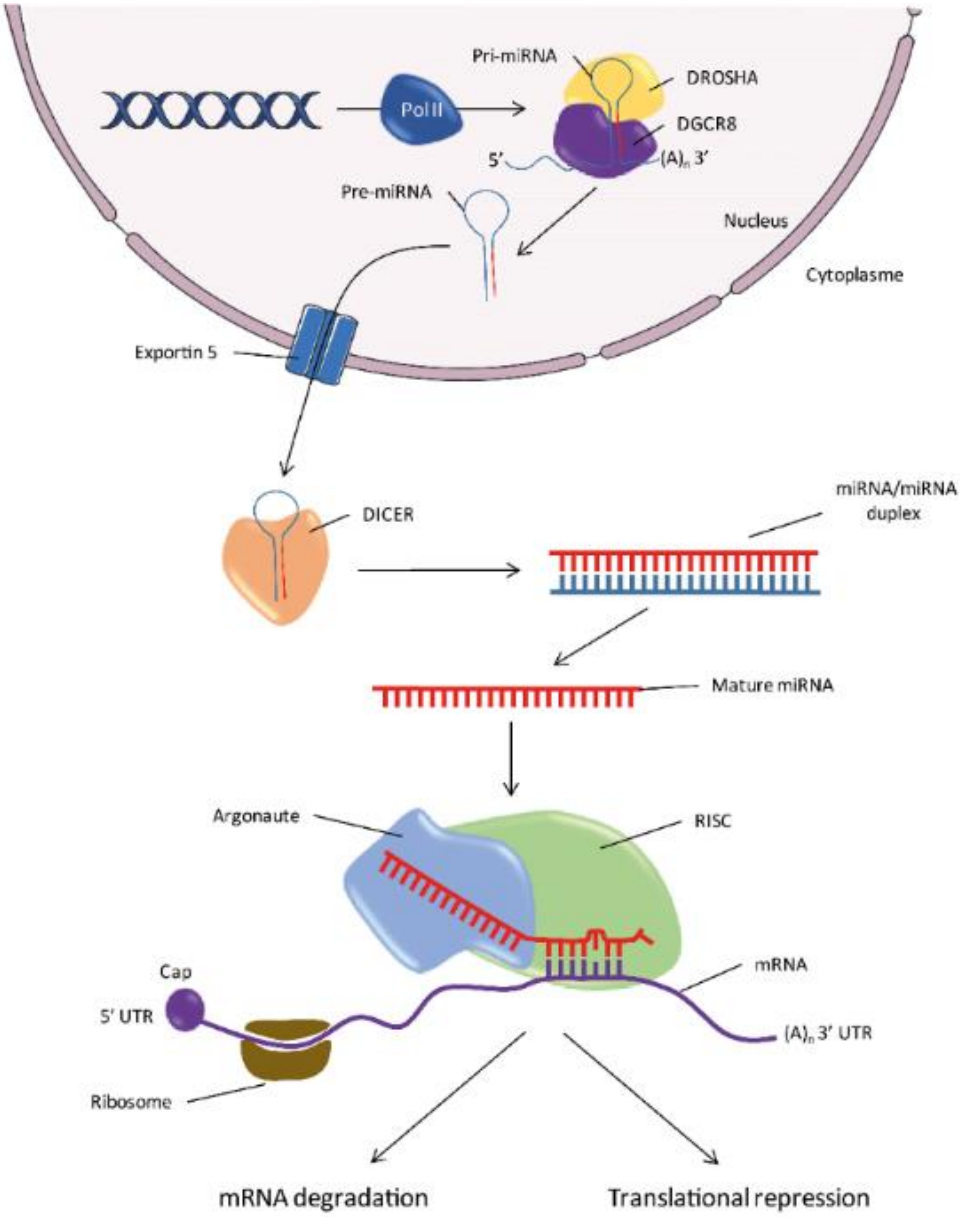

Fig. 6: Biogenesis of miRNAs. Pol II, RNA Polymerase II; pri-miR, primary miRNA; pre-miR, precursor miRNA; RISC, RNA-Induced Silencing Complex; 5′ or 3′UTR, 5′or 3′untranslated region; DGCR8, DiGeorge Syndrome Critical Region 8; (A)n, Polyadenylation. (82)

3.7. miRNA and HCC

miRNAs have been shown to be dysregulated in various cancer types (83). Their roles have also been established in liver development, metabolism, inflammation, fibrosis, infection and tumor development (84). As miRNAs have been shown to be involved in important cellular functions, therefore it is unsurprising that miRNAs appear to be dysregulated in HCC, as shown in both human and animal studies. Mounting experimental evidence indicate that based on their expression pattern miRNAs may also act as tumor suppressors or oncogenes by directly or indirectly targeting the expression of key proteins in cancer related pathways (Table 2) (85).

A tumor suppressor gene is defined as a gene which usually prevents tumor development or tumorigenesis. Common findings from HCC studies suggest that subset of miRNAs are significantly downregulated and may act as tumor suppressors. miR-122, a most abundant liver specific miRNA is downregulated in HCC tumor tissues and cancer cell lines, and overexpression of it has been found to suppress cell proliferation and induce apoptosis in HepG2 and Hep3B cells(86). Other miRNAs such as miR-199 and miR-206 have been shown to inhibit HCC proliferation and metastasis. miR-199 suppresses HCC growth by inhibiting p21-Activated kinase 4, which is known to activate Raf/MEK/ERK kinase, whereas miR-206 inhibits tumor growth by targeting cell cycle regulatory protein CCND1, cMET and CDK6. Several other tumor suppressor miRNAs have been described (87–89).

Several studies have also shown miRNAs to be oncogenic (OncomiR) (89). OncomiRs that are upregulated potentially target the tumor suppressor genes and important signaling pathways, thus regulating the cell proliferation and apoptotic process that is critical for HCC development. For example, miR-21 which is the most commonly overexpressed miRNA in cancer contributes to hepatic steatosis and cancer progression by modulating p53 and Srebp1c pathway via target HBP1 (HMG-box transcription factor 1) (90). miR-224 acts as an oncomiR through the activation of AKT signaling (91). Another miRNA, miR-184 has been shown to upregulate cell cycle progression proteins c-Myc, cyclin D1and phosphorylated RB protein by targeting SOX7, thus increasing the HCC cell proliferation(92).

OncomiRs	**Target(s)**
miR-21	PTEN
	HBP1-p53-SREBP1C pathway
miR-93	PTEN, CDKN1A
miR-106b	DAB2 (disabled homolog 2)
miR-184	SOX7
miR-221	p53
	p27 and/or DDIT4
miR-221/222 cluster	BBC3
miR-224	AKT signaling
Tumor suppressor miRNAs	
miR-122	p53/MDM2
miR-148b	WNT1
miR-193a-5p	NUSAP1
miR-195	CDK6, CCNE1, CDC25A, and CDK4
miR-199a/b-3p	PAK4/Raf/MEK/ERK pathway
miR-199a-5p	HK2
miR-206	CCND1, cMET, and CDK6
miR-766-3p	Wnt3a/PRC1 pathway

Table 2: List of oncomiR's and suppressor miRNAs (89)

3.8. Next generation Sequencing (NGS)

Elucidation of the molecular mechanism underlying TR regulation in human HCC has resulted so far limited and inconclusive. Moreover, due to the limited possibility to identify and diagnose early stages of liver tumor development in humans, the precise sequence of molecular events involved in tumor initiation in not well defined. Since, most of the studies have focused on fully developed HCCs, molecular pathogenesis of HCC cannot be fully under stood.

In this context, miRNAs have been demonstrated to play prominent role cancer development and progression. Very few studies have attempted to address the complete miRNA dysregulation profile in the early stages of tumor development. Among the recent techniques, transcriptomics has been extensively used and have proven to be a valuable tool for understanding cancer mechanisms and identifying important metabolic pathways deregulated in cancer.

Next generation sequencing (NGS) has revolutionized the field of genomic research. Sequencing of the human genome in early 2000s has led to the increased interest in cheap and rapid sequencing technologies. Advancement in the field of genomics and decreased cost per mega base in NGS has brought swift advances to our understanding of evolution, cell biology and microbial environments (Fig. 7). It has enabled the researchers to better understand life at the molecular level. NGS has also enabled the researchers to decode the genetics of human disease as well as in the development of specific preventive, diagnostics and therapeutic strategies. Over the last decade, particularly in the field of cancer, it has had a profound impact on our understanding of cancer genomics. Two large consortia led the way in generating and analyzing NGS data from different cancer types. The Cancer Genome Atlas (TCGA) (93), predominantly using exome sequencing, and The International Cancer Genome Consortium (ICGC) (94), using whole genome sequencing, explored somatic mutations across thousands of cases from >30 cancer types. These consortia combined both sequencing approaches with transcriptional, methylation and protein analyses. NGS has allowed scientists to answer complex questions that were beyond the capacity of traditional DNA sequencing technologies. It has become an everyday tool of research.

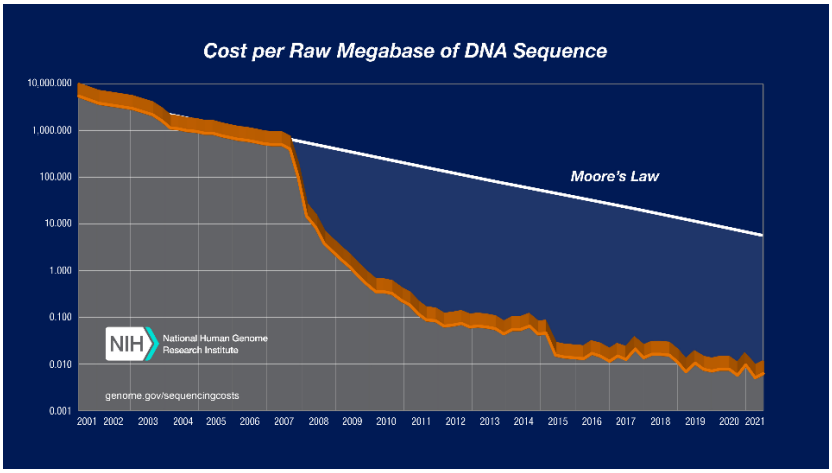

Fig. 7: Sequencing cost per megabase

3.9. Computational analysis of NGS Data

With the rise of NGS data, computational analysis tools have dramatically increased during the past decade. Although the bioinformatics community has responded with novel tools and algorithms to process and interpret this data, many challenges still remain in the area of data management, analysis, security and privacy, ease of use, interpretability, and reproducibility of results.

The ability to reproduce data and results is at the heart of science. The reproducibility of scientific workflows and pipelines is a ubiquitous problem in science(95). It is particularly a major challenge in the areas that heavily rely on computation and data analysis, because of the dependency on heavy computationally intensive tasks and the number of software and system libraries. In recent years, irreproducibility has been a growing concern in the scientific community. Particularly in the field of genomics, scientists have called for rigorous strategies, good data management and best practices for the development and utilization of the computational workflow. International guidelines have been proposed to improve the Findability, Accessibility, Interoperability, and Reuse of digital assets (FAIR) by a consortium of researchers. FAIR guidelines describe the ideal way of storing and sharing research outputs, so that they can be easily accessed, understood exchanged, and reused. Initially developed for the academic world, these principles are gradually becoming a reference both at state and industry levels (96,97).

Analysis of the transcriptomics data can be tricky, and often requires substantial expertise in bioinformatics. Prior to the final analysis, the raw data needs to be processed through number of steps. Broadly these steps can be divided in to 3 main categories: 1) quality control 2) alignment and 3) quantification. Bioinformatic workflows are generally employed to automate these steps. A number of workflow managers are available to help the researchers preprocess their data. Recently, several standalone and web-based tools have been proposed as a solution to counter the reproducibility problem. Example of such tools in genomics include containerization of bioinformatic tools using docker and singularity, and workflow managers such as Nextflow, Snakemake, Galaxy, etc.

Containerization method allows bundling of applications with all its dependencies using languages such as Python and R to the operating system itself. It has rapidly gained popularity among the scientist and researchers, and the way they develop, deploy and exchange scientific software (98). However, issues such as limited availability of tools, security, isolation and networking issues don't make containerization the best choice for application deployment (99). Web based tools such as Galaxy offers graphical user interface (GUI) for constructing workflows for next-generation sequencing and gene expression data analysis. Nevertheless, using Galaxy with big data requires local installation, and analysis is only allowed with well-implemented tools. Installation of new tools can only be done by the users with admin privileges (100,101) .

Two popular workflow management projects Snakemake (102) and Nextflow (103) are currently being used as alternatives to containers and web-based solutions. Written in Python and Groovy respectively, both offer flexibility of adding any tool, scalability, automatic parallelization of jobs, portability, support for Conda environment and extensive documentation.(104). They are emerging as a solid choice for developing scientific workflows.

Here, we describe two automated, scalable, and reproducible Snakemake based pipelines called RIDE (RNA Differential Expression) and SRIDE (small RNA Differential Expression) for performing transcriptome and microRNA analysis respectively.

4. AIM OF THE STUDY

Primary liver cancer is the sixth most commonly diagnosed cancer and is the third largest contributor to cancer mortality. Benefits from present treatment options are still disappointing, as they extend the median life expectancy of patients by only few months. Thus, it is mandatory to find alternative treatment options. Experimental and clinical studies revealed a status of severe local hypothyroidism in rat hepatic preneoplastic lesions, and in human HCCs, suggesting that this condition may represent a favorable event for HCC development

Previous research conducted in our laboratory demonstrated that the reactivation of THR axis upon T3 treatment was associated with regression of preneoplastic and neoplastic lesions in the Resistant Hepatocyte rat HCC model, thus suggesting a therapeutic role of THR agonist for HCC.

Based on this premise we performed a comprehensive and comparative miRNomic and transcriptomic analysis of hepatic preneoplastic lesions of rats. The aims of present study were the following:

- Investigate mRNA expression in preneoplastic lesions without and after T3 treatment.
- Analyze the miRNoma of preneoplastic lesions without and after T3 treatment.
- Perform Integrative Analysis of miRNA-mRNA expression profiles and identify the modulated metabolic pathways.
- Validate selected microRNA in cell lines transduced with THRB and with or without T3 treatment.
- Implement automated, scalable, and reproducible workflows for processing raw NGS data.

5. MATERIALS AND METHODS

5.1. Resistant-Hepatocyte (R-H) model. All animal procedures were approved by the Ethical Commission of the University of Cagliari and the Italian Ministry of Health. Male Fischer F-344 rats (100-125g) were purchased from Charles River (Milano, Italy). Animals were subjected to the Resistant-Hepatocyte (R-H) model of hepatocarcinogenesis, consisting of a single intraperitoneal dose of diethylnitrosamine (150 mg/kg body weight, DEN, Sigma,) followed by a brief (2 weeks) promoting procedure with 2-acetylaminofluorene (2-AAF, Sigma) and a two-thirds partial hepatectomy (PH). Rats were then switched to a basal diet all throughout the experiment and sacrificed ten weeks after DEN administration. One group of animals was fed a T3-supplemented diet (4 mg/kg of diet) for 4 days starting 5 weeks after 2-AAF withdrawal. Rats kept on a basal diet were used as a control group. Another group of animals exposed to the R-H protocol was maintained on basal diet for 10 months, a time when all rats developed HCC. Animals were then split into two groups; one group was fed T3 supplemented diet for 1 week while the other was kept on basal diet. Histologic classification of preneoplastic nodules and HCCs was performed as previously described.

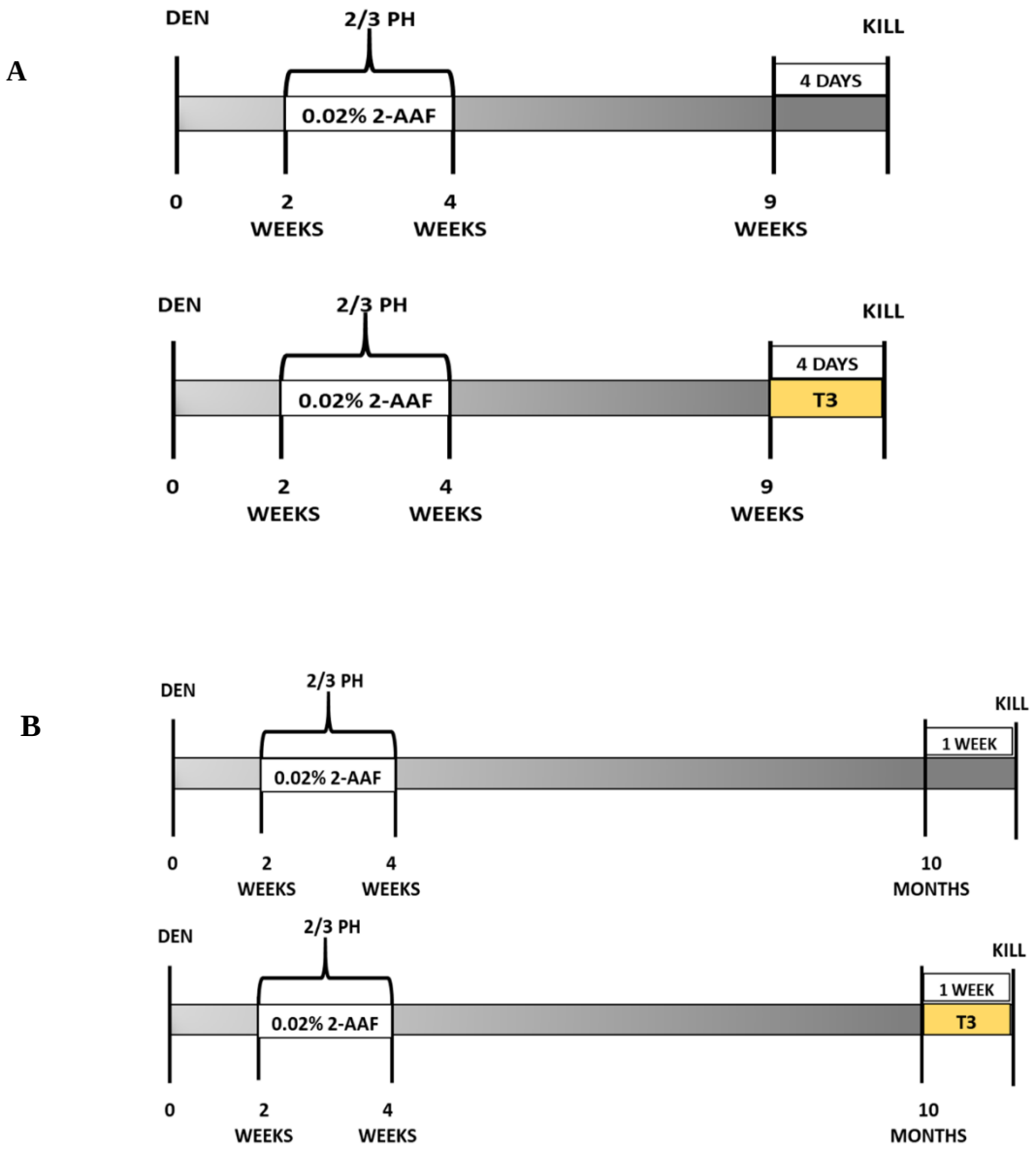

Fig. 8. Experimental Protocols. **A)** Rats were given a single dose of DEN (150 mg/kg bw) followed by a 2-weeks feeding of 2-acetylaminofluorene (0.02%) and a two-thirds partial hepatectomy (PH). Animals were then switched to a basal diet. Five weeks after 2-AAF withdrawal, one group of rats was fed a T3-supplemented diet (4 mg/kg of diet) for 4 days. Rats kept on a basal diet were used as a control group; **B)** Rats given a single dose of DEN and then exposed to 2-AAF + PH as in A and were switched to basal diet till 10 months from DENA. One group of animals was fed a T3-supplemented diet (4 mg/kg of diet) for 7 days prior to sacrifice. Rats kept on a basal diet were used as control group.

5.2. Histology and immunohistochemistry

5.2.1. Tissue Preservation

Immediately after the sacrifice, livers were cut in several pieces and preserved in different ways to carry out multiple analysis. For immunohistochemistry analysis, liver sections were fixed in 10% formalin, embedded in paraffin and stored at room temperature (RT). Other sections were immediately frozen in liquid nitrogen-cooled isopentane and preserved at -80°C for future molecular analysis and cryosectioning.

5.2.2. Hematoxylin and Eosin (H&E) staining

4µm thick paraffin-embedded liver sections were deparaffinised in Bioclear (BioOptica, Milan, Italy) for 30 minutes and hydrated in a decreasing series of alcohol. Sections were then incubated in Carazzi Hematoxylin for 20 minutes and after several washes in tap water, stained in 1% acidified alcoholic eosin for 14 seconds. Sections were then dehydrated through ascending alcohol series, cleared with Bioclear, air-dried and then mounted using synthetic mounting and cover slipped.

For cryosections, 6µm thick sections were used. Samples were previously fixed in 10% buffered formalin for 1-6 hour and washed in distilled water for 5 minutes (two washes). Following this, similar protocol was adopted as mentioned above.

5.2.3. Glutathione S-transferase (GST-P) staining

Formalin fixed sections of 4µm thickness were deparaffinized in Bioclear for 1 hour, followed by rehydration by immersing the slides in decreasing series of alcohol. Next, samples were washed twice in phosphate buffered solution (PBS), and blocking of unspecific antibody binding sites was performed in 10% normal goat serum (Abcam,ab7481) for 30 minutes at RT. Overnight incubation was performed with 1:1000 diluted rabbit anti-GSTP primary antibody (MBL, 311) at 4°C in humid chamber. Next day, to block endogenous peroxidase activity, slides were incubated in 0,5% hydrogen peroxide (31642, Sigma-Aldrich) in distilled water for 10 minutes, followed by secondary antibody incubation. Sections were incubated with anti-rabbit Horseradish Peroxidase (HRP) secondary antibody (A0545, Sigma-Aldrich) at 1:300 dilution for 40 minutes at RT. Positive binding reaction was visualized using 3.3'-diaminobenzidine (DAB) (Sigma-Aldrich) for

6 minutes at RT. Afterwards, slides were counterstained with Harris Haematoxylin Solution (Bio-Optica), dehydrated through graded alcohols, cleared and coverslips were mounted with synthetic mounting media.

Immunostaining was also performed in 6µm thick cryosections using the same protocol, apart from the clearance and rehydration steps, substituted by a 6-hour fixation in 10% buffered formalin followed by 15 minutes washing in distilled water.

5.2.4. KRT-19 and NQO1 Staining

4µm thick tissue sections were deparaffinized in Bioclear for 1 hour and rehydrated by immersing the slides in decreasing series of alcohol. Following two washes in PBS, antigen retrieval in Sodium Citrate Buffer was performed. Details regarding retrieval, primary and secondary antibody dilutions are reported in Table 3.

Staining	**Retrieval Conditions**	**Primary antibody**	**Secondary antibody**
KRT-19	2X6 min MWO 700W	NBP100-687 (Novus-Biologicals) 1:400 at 4°C overnight incubation	Dako anti-rabbit, (K4003) 60min RT
NQO1	4X5 min MWO 700W	Mouse (ab28947, Abcam) 1:100 At 4°C overnight incubation	Dako anti-rabbit, (K4003) 60min RT

Table 3. Details regarding retrieval, primary and secondary antibody dilutions used in the study.

5.3. Laser-capture Micro-dissection (LMD)

Sixteen-µm-thick serial frozen sections of rat livers were attached to 2-µm RNase free PEN-membrane slides (11505189, Leica, Wetzlar, Germany). Microdissection (Leica, LMD6000) was preceded by a H&E and GSTP staining on serial sections. RNA and miRNA isolation. Total RNA was isolated with the mirVana miRNA isolation kit (cat.# AM1560, Life Technologies) from 3 livers of untreated rats, and preneoplastic nodules from rats treated with T3 (6 nodules) or not

exposed to the hormone (5 nodules). As to HCC, miR expression was evaluated in 11 HCCs from rats subjected to 1-week T3 feeding or 10 HCCs from rats not exposed to the hormone. Gene expression analysis was also performed on some of the microdissected HCCs.

5.4. Deep sequencing

For RNA and miRNA sequencing experiments, indexed libraries were prepared using 100 ν g of total RNA as starting material, with a TruSeq Stranded Total RNA Sample Prep Kit and QIAseq miRNA Library Kit (Illumina Inc.) respectively. RNA was quantified by Nanodrop spectrophotometer (Thermo Scientific) and its integrity was evaluated by Agilent Bioanalyzer 2100 (Agilent Technologies, CA, USA). Only RNA samples with a RIN (RNA Integrity Number) ≥ 7 were included for library preparation. Libraries were prepared according to manufacturer's protocol. Following, libraries were sequenced (single-end, 75 cycles) at a concentration of 8 pM/lane on the HiSeq 3000 platform (Illumina Inc.) at the CRS4 (Center for Advanced Studies, Research and Development in Sardinia) facility.

5.5. qRT-PCR

Gene expression was assessed in HCCs by qRT-PCR using specific Taqman probes (Nqo1,Rn00566528_m1; Gstp1, Rn00561378_gH; Dio1, Rn00572183_m1; Krt-19, Rn01496867_m1). Each sample was run in triplicate and gene expression analysis of Glyceraldehyde 3-phosphatase dehydrogenase (Gapdh) was used as reference gene. cDNA was synthesized using the TaqMan® MicroRNA Reverse Transcription Kit. qRT-PCR amplification was performed with the reverse transcription product, TaqMan® 2X Universal PCR Master Mix, No AmpErase ®UNG. miR primers used were: I-miR-185 TM:002271; hsa-miR-425-5p TM:001516; mmu-miR-140 TM:001187; hsa-miR-27a TM:000408; rno-miR-224 TM:464298. Probe mix was from Thermo Fisher Scientific. The endogenous control U6 (U6 snRNA TM:001973) was used to normalize miRNA expression levels.

5.6. Cell cultures and in vitro experiments

HepG2 cell line was obtained from ATCC (Manassas, VA, USA). Mahlavu cells were a kind gift of Dr. N. Atabey; they were routinely cultured in essential aa supplemented-MEM and DMEM medium (Sigma-Aldrich; Saint Louis, MO, USA), respectively, in the presence of 10% fetal bovine serum P/S (100U/ml Penicillin, 8 100mg/l Streptamicin), and L-Glutamine (2mM) (Lonza,

Basel, Switzerland) and incubated at 37°C in a 5% CO2-95% air-humidified atmosphere. Cells were transduced with either a lentiviral vector expressing THRB gene (GeneCopoeia, cat. EX-T9450-Lv186) or an empty lentiviral vector. Both cell lines were seeded in the presence or in the absence of 100 nM triiodothyronine (Sigma) for 48 hours. Analysis of miRNA expression was performed as described 11. Briefly, the expression of miR-140 (hsa-miR-140-3p, #002234), miR-185 (has-miR-185-5p, #002271), miR-425(hsa-miR-425-5p, #001516), miR-421(has-miR-421, #002700) and miR-224 (hsa-miR-224-5p, # 483106_miR) in Mahlavu and HepG2 cells, was performed starting from equal amounts of total RNA/ sample (50ng) using the specific Taqman microRNA assay or TaqMan Advanced miRNA Assays kits (Applied Biosystems). MiRNA expression was calculated as fold change using the delta-delta CT method and RNU48 as endogenous control. miR-191-5p, consistently expressed in HepG2 cells was used to normalize miR-224-5p levels (105).

5.7. Bioinformatic Analysis

Implementation

5.7.1. Snakemake as framework

Snakemake is a python-based workflow management tool. Compared to other tools, Snakemake enables the user to conduct analysis that have all the properties of sustainability, transparency, reproducibility, and adaptability. Central idea of Snakemake is that workflows are segmented into several steps so-called *rules*. The output files from a *rule* are used as input for the next task in the workflow. Other features that make Snakemake an ideal choice for scientific workflow management is readability, portability, scalability, traceability, flexible package management and documentation. In order to obtain reproducible results, Snakemake rules are executed within isolated software environments created with Conda(106). Conda is an open-source package and environment management system that helps in creating independent virtual environments and installing specific versions of software packages and their dependencies. Upon execution of a Snakemake based pipeline, Conda package manager automatically downloads and deploys specified versions of software packages.

RIDE

5.7.2. RIDE Pre-processing

Raw FASTQ files are preprocessed by removal of 3' adaptor using trim-galore tool (107). Remaining arguments were kept at default for processing the samples. Adaptor free sequences are further processed for alignment and quality control.

5.7.3. RIDE Quality Control

Initial quality control steps include processing of raw and adapter trimmed samples using FASTQC (108). Additional quality control statistics such as mapped reads distribution, nucleotide composition bias, PCR bias and GC bias is collected by RseQC (109). All the statistics are summarized in to one html file with MultiQC tool (110).

In order to comprehensively evaluate the quality of the RNA-seq data through RSEQC tool (109), the pipeline performs additional indexing and alignment using STAR (111). A genome index is created from the reference genome (available from https://genome-euro.ucsc.edu/cgi bin/hgGateway?redirect=manual&source=genome.ucsc.edu) followed by mapping of the reads. Finally, the mapped bam file is indexed using samtools and piped in to quality control tools.

5.7.4 RIDE Quantification

RIDE pipeline quantifies the abundance of transcripts using Kallisto (112), a tool that utilizes the pseudoalignment method to match the reads to the reference transcriptome of known coding and non-coding transcript sequence. Indexing is performed on the reference transcriptome (available from https://www.ensembl.org/index.html), followed by transcript quantification. Quantification of the paired end reads run on default Kallisto parameters, whereas, single end reads are processed using following parameter—"--single -b 30 -l 280 -s 80", representing the number of bootstrap sampling 30, estimated average fragment length 280 and estimated standard deviation of fragment length 80. Fig. 9 shows a schematic representation of the RIDE workflow.

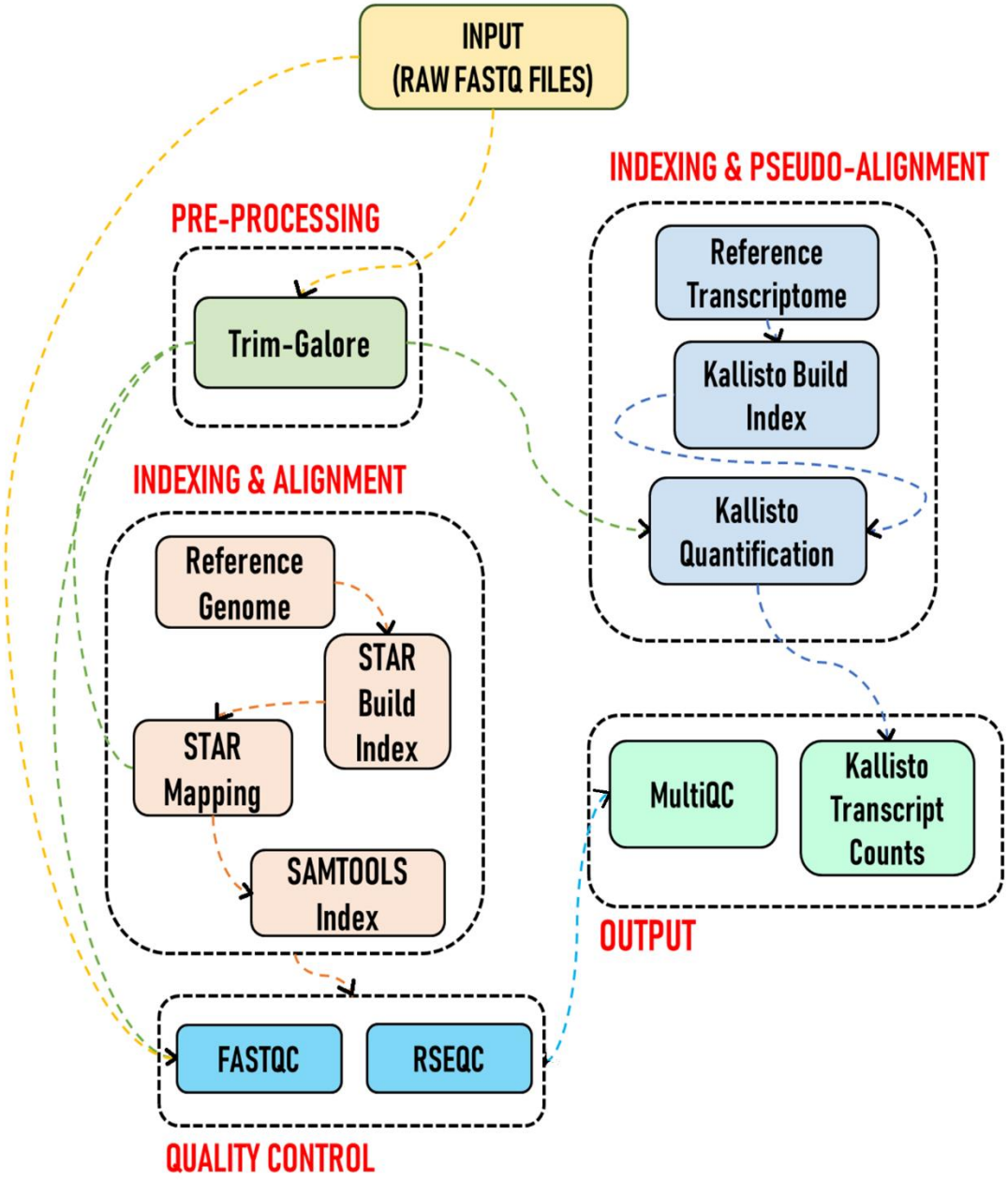

Fig. 9. A Schematic workflow of RIDE

SRIDE

5.7.5. SRIDE Pre-Processing

Default preprocessing steps include UMI removal and trimming of adaptors. FASTQ files without UMI can also be analyzed by specifying the parameter in "config file". We used UMI-tools (113) , a software toolbox for dealing with UMI containing raw FASTQ files. Currently, the workflow supports processing of reads prepared with QIAseq miRNA library kit. The mock sequence of a standard UMI containing read has been shown in Fig.10.

Following UMI extraction, FASTQ files then undergo trimming using Trim -galore tool, which removes low quality bases and adapter sequences from the 3' end of the reads. Clean reads are then ready for quality control and alignment.

Fig 10. Mock Sequence of a raw miRNA read.

5.7.6. SRIDE Quality Control

The pipeline employs 3 quality control tools for the identification of low-quality and contaminated samples. Quality of the raw reads and trimmed reads is assessed using FASTQC (v0.11.3) tool (https://www.bioinformatics.babraham.ac.uk/projects/fastqc/). Furthermore, each trimmed sample is characterized by profiling the sequencing quality, length, depth, and complexity using mirTrace. In addition to the quality control analysis, the pipeline can accurately detect samples with common sequencing contaminants and cross-clade contaminants using FastQ-Screen and mirTrace tools respectively.

5.7.7. SRIDE Quantification

The trimmed reads are then aligned using the ultrafast and memory-efficient short read aligner tool Bowtie. The default configuration of bowtie runs on parameters- "-v2 -m10 -a", where 2 mismatches in the bases are allowed and refrains bowtie from reporting any alignments for reads having more than 10 reportable alignments. "-a" in the parameter instructs Bowtie to report all valid alignments, subject to the alignment policy: -v 2.

The aligned reads from bowtie are piped in to *samtools index* followed by removal of the PCR duplicates using UMI-dedup tool. Currently, the deduplication step runs on one parameter, i.e—"--method=unique", which identifies group of reads that share the exact same UMI (if present)". The statistics of the deduplication run is not collected in order to avoid excessive memory usage and crash.

The final step of the pipeline involves counting of each miRNA aligned to the reference sequence. The aligned and deduplicated reads are counted using *htseq-count* tool: Given a GTF of GFF file containing a list of genomic features, the tool counts how many reads map to each feature. These counts are then further used for differential expression analysis. Fig. 11 shows a schematic representation of the SRIDE workflow

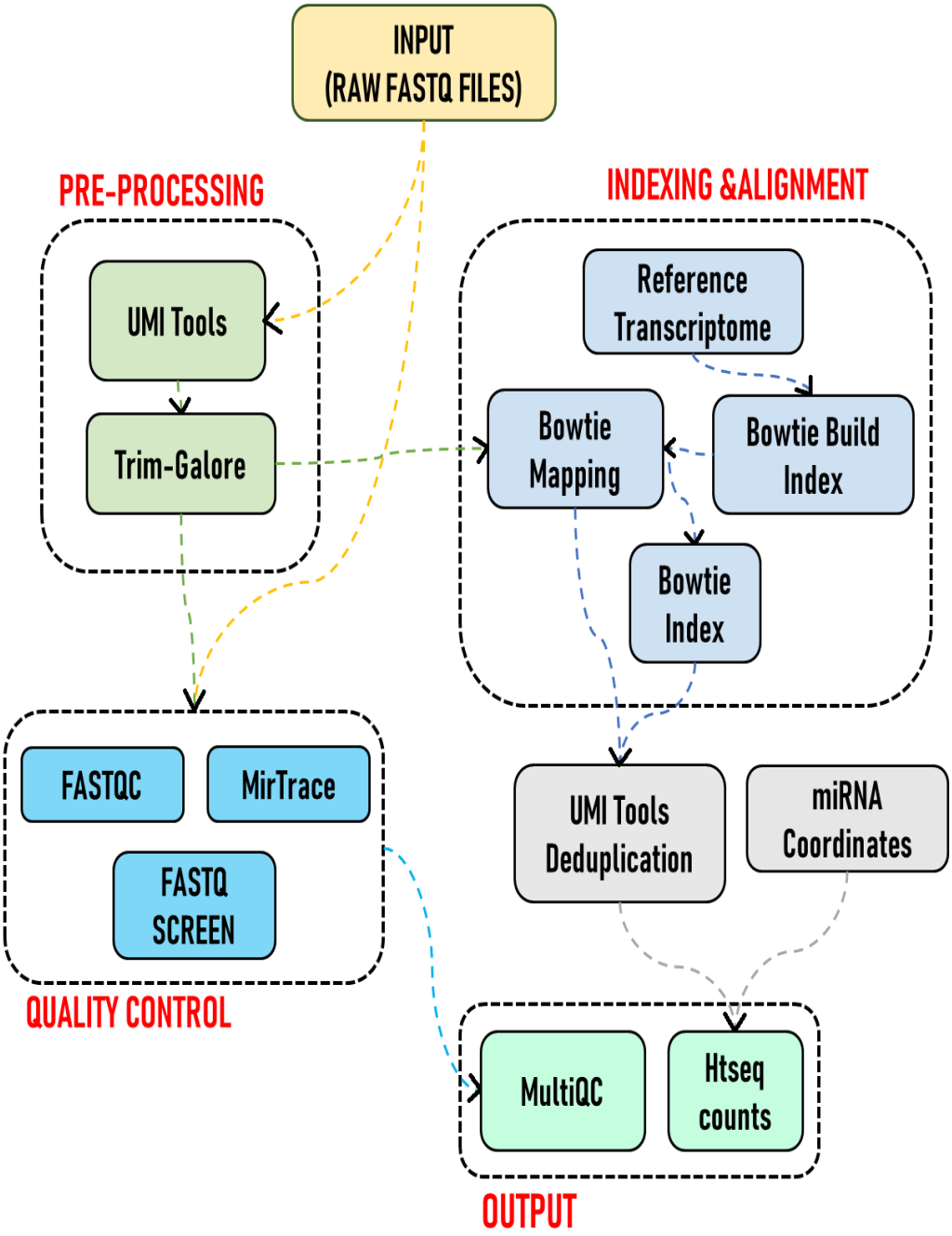

Fig. 11. A schematic workflow of SRIDE

5.7.8. Configuring and Running the Workflows

RIDE and SRIDE are free, open source, and released under the GNU General Public License v3.0. Source code of both the pipelines are freely available at CRS4's GitHub repository (https://github.com/solida-core).

Both the pipeline automatically downloads and installs all the required dependencies. The user is only required to install Python (https://www.python.org/downloads/), Git(https://git-scm.com/downloads), Conda (https://conda.io/projects/conda/en/latest/user-guide/install/index.html) and Snakemake (https://snakemake.readthedocs.io/en/v5.6.0/getting_started/installation.html) in their system. Additional information about the installation procedure can be accessed on their respective tutorial pages.

5.7.9 Workflow Output

We evaluated both the workflows using multiple sequencing datasets (both SE and PE) from different organisms as input. Here we provide snapshots from the summarized QC report generated after the successful execution of the workflows. The MultiQC report provides a number of useful metrics which enable the users to identify any issues with the data and/or the parameters. It also alerts the users if there is a presence of contamination or systemic biases, etc.

By default, counts file generated by the workflows are stored in "delivery" folder, however, it can be user modified to store them in different location. Log files are created for each step, including information about relevant software version and parameters used (wherever applicable). Additional statistics including the output from trimming tools, sequence quality, contamination etc. is merged in to single html file by MultiQC tool. The output can be accessed under the folder name 'qc'.

For SRIDE and RIDE workflows, FastQC checks the quality of the sequencing reads before and after trimming the raw FASTQ files. Users are required to check the metrics and decide whether further trimming is needed (Fig. 12 A). Trimming should not be performed if the quality of the reads is good enough since it would lead to the loss of information.

For RIDE, the percentage of each read that are successfully (pseudo)aligned to the refence transcriptome using Kallisto tool can be visually analyzed in the final report. Low percentage of pseudoalignment indicates possible rRNA contamination or low-quality reads (Fig 12 C).

Additionally, DNA contamination in the reads can be visualized from the metrics generated by ReSeQC read distribution tool. This tool calculates how mapped reads are distributed over genomic features. A good RNA seq experiment generally has as many exonic reads as possible (CDS_Exons). A large number of intronic reads could be indicative of DNA contamination in the sample or some other problem (Fig 12 D).

For SRIDE workflow, the percentage of reads aligned to miRNA sequence can be accessed with mirTrace plot Low percentage of miRNA read alignment indicates tRNAs, rRNAs, and synthetic adapter sequence contamination (Fig 12 E).

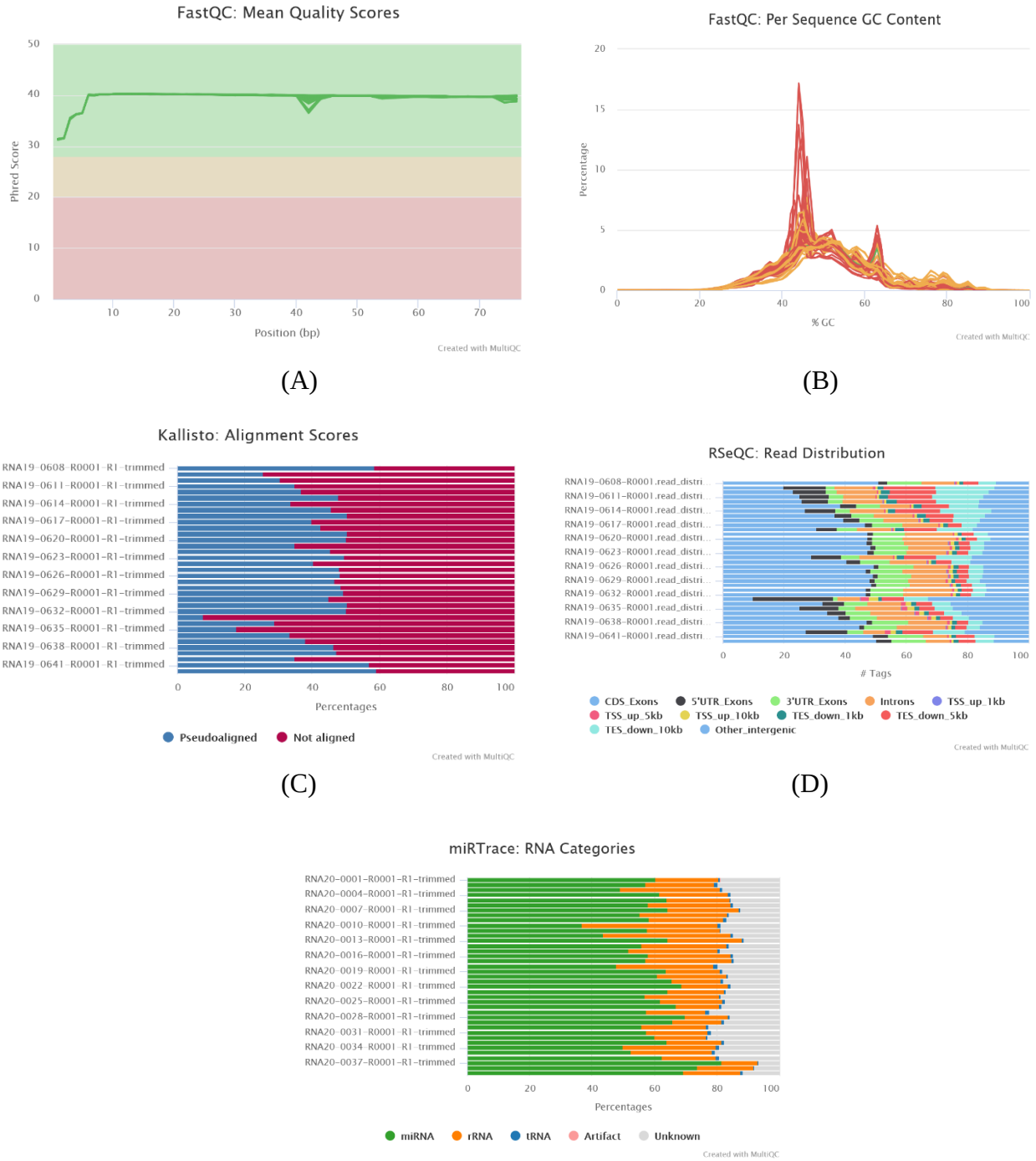

Fig. 12. MultiQC report of raw reads. **A)** The mean quality value across each base position in the read. **B)** The average GC content of reads. A normal random library typically has a roughly normal distribution of GC content **C)** Kallisto transcript quantification of each sample. **D)** RSEQC sample read distribution **E)** mirTrace: (114) detected RNA categories of each sample.

5.7.10. Differential Expression Analysis

For RNA-Seq, Kallisto transcript counts were converted to genes counts using the R package Txiimport (115), whereas, miRNA count table objects were directly imported in to the R Studio. DESeq2 package was used to perform statistical tests and differential gene/miRNA expression analysis between groups. Low abundance genes were filtered out, and only those having a mean raw count > 5 in more than 50% of the samples were included. Following normalization, count data were transformed for visualization using the rlog function of DESeq2 (116). Genes with fold change cutoff ≥ 1.5 and miRNAs with fold change cutoff ≥ 1.4 along with Benjamini-Hochberg (BH) adjusted false discovery rate (FDR) < 0.05 were considered significant and were taken into consideration for further analysis.

5.7.11. Visualization

Heatmaps were generated using the pheatmap package in R.100% of the genes/miRNA's were used for clustering and visualization purpose. Principal component analysis (PCA) plot was generated using the plotPCA function in DESeq2 package. Volcano plots were generated with EnhacedVolcano R package (117).

5.7.12. Gene Set Enrichment, Pathway Analysis and miRNA target Filter

In order to summarize high dimensional gene/miRNA expression data in terms of biologically relevant sets we utilized Ingenuity Pathway Analysis (IPA) tool (Ingenuity Systems, Mountain view, CA, USA). Differentially expressed genes and miRNA's passing the cutoff value were uploaded and submitted for IPA core analysis. Core analysis was performed to identify significantly altered canonical pathways and disease and biological functions across the groups. Two distinct statistical analyses were performed during the core analysis. A right tailed fisher's exact test was used to determine the probability that each biological function enriched in the dataset is statistically significant and not due to the chance alone ($p < 0.05$). Additionally, Z-score was calculated to provide predictions about upstream or downstream biological process. In the present study, -log(p-value) of 1.3 (corresponding to 0.05) and z score of ≥ 2 and ≤ -2 was considered for further analysis.

For identifying the target genes of differentially expressed miRNA, microRNA Target filter module was used. Default settings were used while predicting the miRNA target.

5.7.13. Statistics

Data are expressed as mean ± standard deviation (SD). Analysis of significance was done by Student's t-test and by One-Way ANOVA using the GraphPad software (La Jolla, California).

5.7.14. Data Availability

The Source Code of miRNA and gene analysis workflows can be freely accessed at Github: https://github.com/solida-core/ride,https://github.com/solida-core/sride. The datasets supporting the conclusions of this article are available in the Sequence Read Archive (SRA) repository, BioProject ID PRJNA750113, http://www.ncbi.nlm.nih.gov/bioproject/750113.

6. RESULTS

6.1. Effect of T3 on preneoplastic nodules obtained with R-H model

Thyroid hormones have prominent effects on hepatic fatty acid, cholesterol synthesis and metabolism. Association between thyroid hormones and changes in body weight and liver weight has been reported in several studies (114). In order to analyze the effect of T3 on preneoplastic nodules, animals were subjected to R-H model of hepatocarcinogenesis. The model consisted of animals treated with single intraperitoneal dose of diethylnitrosamine followed by a brief promoting procedure with 2-AAF and a two-thirds partial hepatectomy. Rats were then switched to a basal diet all throughout the experiment and sacrificed ten weeks after DEN administration. One group of animals was fed a T3-supplemented diet for 4 days starting 5 weeks after 2-AAF withdrawal. Rats kept on a basal diet were used as a control group. Another group of animals exposed to the R-H protocol was maintained on basal diet for 10 months, a time when all rats developed HCC. Animals were then split into two groups; one group was fed T3 supplemented diet for 1 week while the other was kept on basal diet. Among the groups compared (Control, Nodules, Nodules+T3) 10 weeks after DENA (according to the R-H protocol), no significant change in body weight was observed (Fig. 13 A). T3 treatment for 4 days was associated with significant decrease in liver and liver to body weight ratio compared to T3 untreated ad control animals . (Fig 13 B, C)

As described previously(118), treatment with T3 for a week induced a rapid and quantitatively important (ca 70%) regression of preneoplastic nodules when compared to untreated preneoplastic nodules. To investigate the molecular changes causing this regression we sacrificed the animals 4 days after T3, a time when the number of preneoplastic lesions is still similar to that of untreated rats (Fig. 13 D, E)

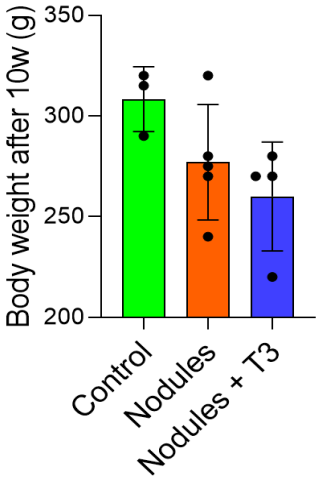

(A)

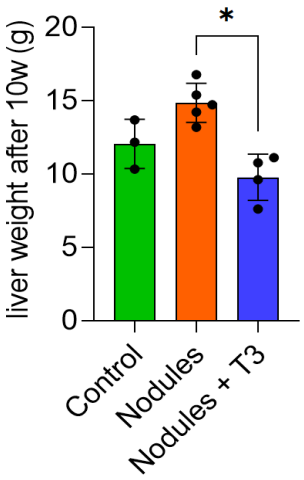

(B)

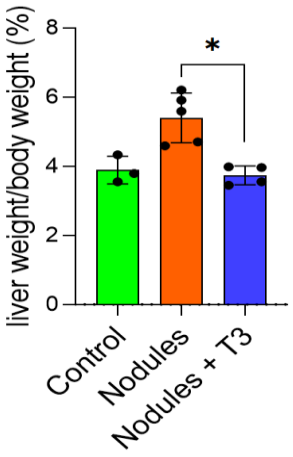

(C)

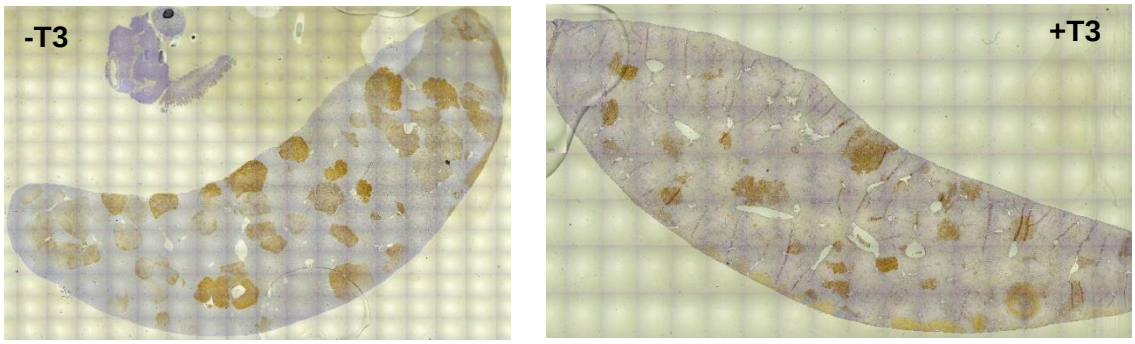

(D)

(E)

Experimental Group	**GSTP-positive nodules/cm^2**
Nodules	27.5
Nodules + T3	25.1

Fig. 13 (A) Body weight; **(B)** liver weight; **(C)** liver weight/body weight ratio. Groups were compared using unpaired two-tailed Student's t-test and non-parametric Mann–Whitney U Test. * $p < 0.05$. **(D)** A representative picture of GSTP immunohistochemical staining of preneoplastic lesions of untreated (-T3) or 4-day T3 treated animals (+T3); **E)** Number of GSTP-positive

preneoplastic nodules in rat livers subjected to the R-H protocol and then treated or not with T3 for 4 days.

6.2. Gene expression analysis and identification of most deregulated pathways in preneoplastic nodules obtained with R-H model

Gene expression profiling was performed using NGS in the same samples used for miR-analysis. A total of 4599 differentially expressed genes (fold-change ≥ 1.5, FDR < 0.05) were identified in nodules vs. control livers: 2372 genes were up-regulated and 2227 were down-regulated. Similar to what was observed for miRNAs, unsupervised hierarchical cluster analysis stratified control livers and preneoplastic nodules into two separate groups (Fig. 14A) and PCA separated the samples according to two groups (Fig. 14B). Ingenuity pathway analysis (IPA) revealed that the top 5 most dysregulated pathways were LPS/IL-1-mediated inhibition of RXR function, FXR/RXR activation, Mitochondrial dysfunction, Nrf2-mediated oxidative stress response and Oxidative phosphorylation (Fig. 14C).

To identify a possible correlation between miRNAs and genes differentially expressed in preneoplastic nodules vs. control livers, we investigated miRNAs potentially targeting genes dysregulated in our transcriptomic analysis using microRNA target filter module of IPA. Of particular interest was the finding that several miRNAs targeting genes involved in the most modified pathways (i.e. Nrf2 pathway and oxidative phosphorylation) were inversely regulated according to their target genes. Indeed, 29 miRs predicted to target genes involved in the strongly activated Keap1-Nrf2 pathway were down-regulated in preneoplastic nodules; conversely, 18 miRs up-regulated in the nodules were reported to target genes involved in Oxidative phosphorylation, a pathway profoundly down-regulated in preneoplastic lesions (Fig. 15 A, B).

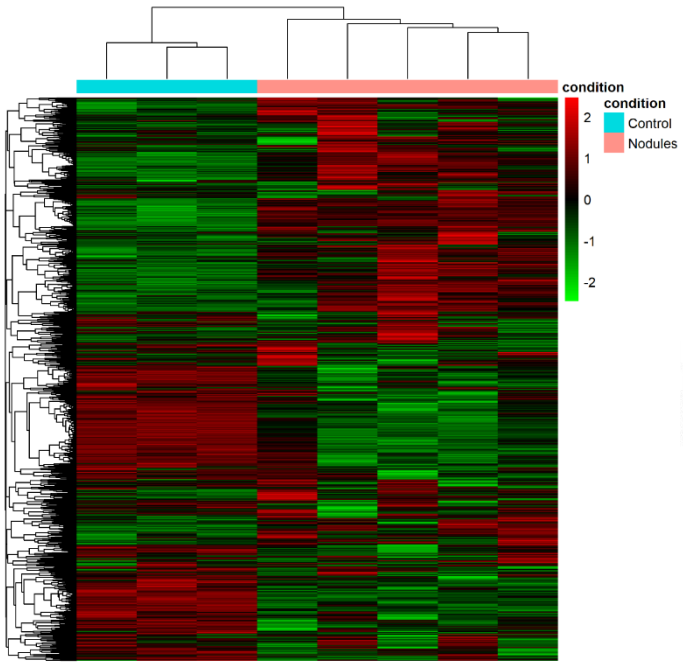

(A)

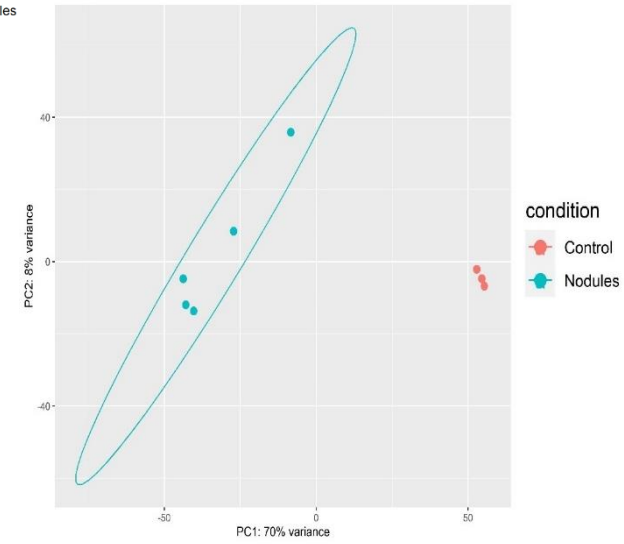

(B)

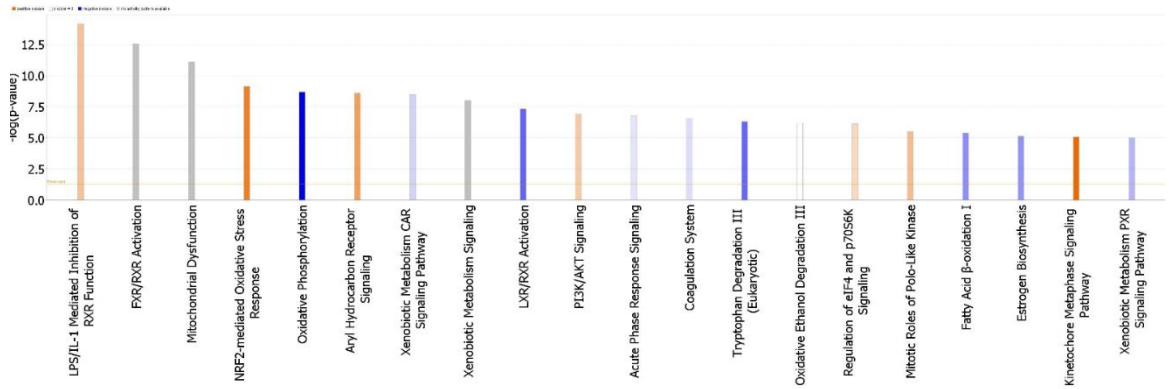

(C)

Fig. 14 A) Hierarchical clustering of genes in preneoplastic lesions (nodules), and control samples. Each row represents the expression of a gene and each column a sample. Red and green colors represent higher or lower mRNA expression levels (median-centered), respectively; **B)** PCA of genes in preneoplastic lesions (nodules), and control samples; **C)** Canonical pathway analysis in preneoplastic lesions (nodules), and control samples.

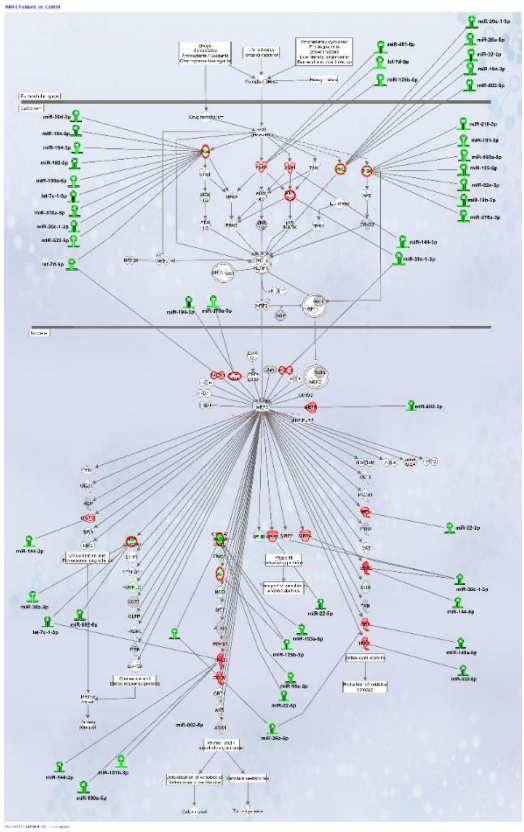

(A)

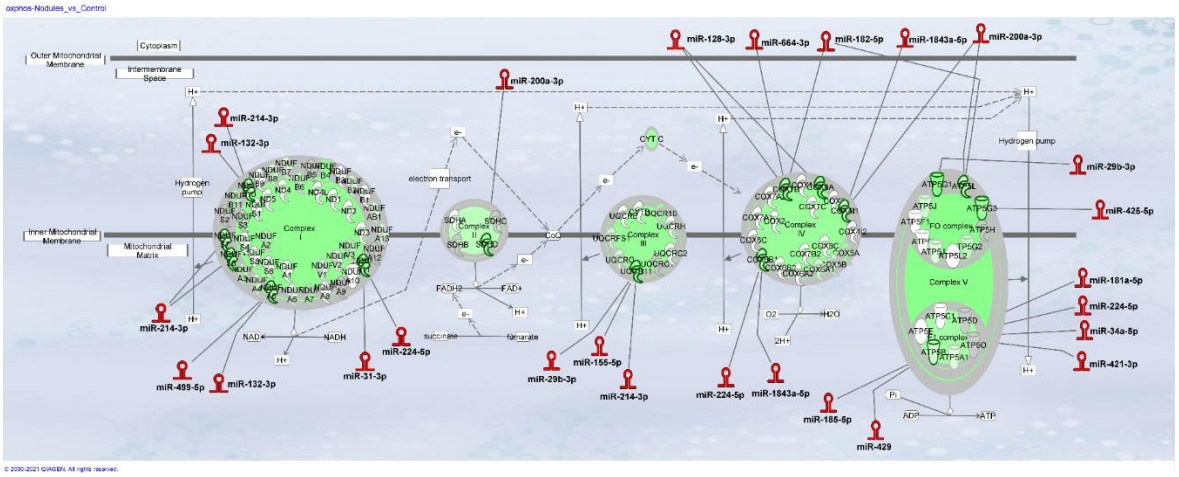

(B)

Fig. 15 A) IPA analysis of the Nrf2 oxidative stress response pathway and **B)** the Oxidative Phosphorylation pathway (OXPHOS) in the early steps of hepatocarcinogenesis. Hairpin loop structures represent miRNAs. (Red: Up-regulated, Green: Down-regulated). Edges connect miRNAs and putative target genes predicted by TargetScan/TarBase/miRecords and Ingenuity Expert Findings.

6.3. Effect of T3 treatment on gene expression profile of preneoplastic nodules

To identify the potential transcriptional changes induced by T3 treatment in preneoplastic nodules, we performed transcriptomic analysis. A total of 2903 differentially expressed genes (fold-change 1.5, FDR < 0.05) were identified in T3-treated nodules, of which 1269 genes were up-regulated and 1634 were down-regulated. Unsupervised hierarchical cluster analysis stratified again untreated nodules and T3-treated nodules into two clearly distinct clusters (Fig. 16A) and PCA separated the samples according to the two groups (Fig. 16B). Disease and biological function analysis of the differentially expressed (DE) genes revealed remarkable enrichment in several functional categories that were reversed upon T3 treatment (Fig. 16C). Top 5 categories down-regulated upon T3 treatment were Growth of tumor, Cell movement, Migration of cells, Microtubule dynamics and Organization of cytoplasm. Differentially expressed genes were also categorized based on Canonical Pathways. The two most significantly dysregulated pathways upon T3 treatment were Oxidative Phosphorylation and NRF2-mediated Oxidative Stress Response, two pathways dysregulated, but in the opposite direction, in nodules vs. control livers (Fig. 16D).

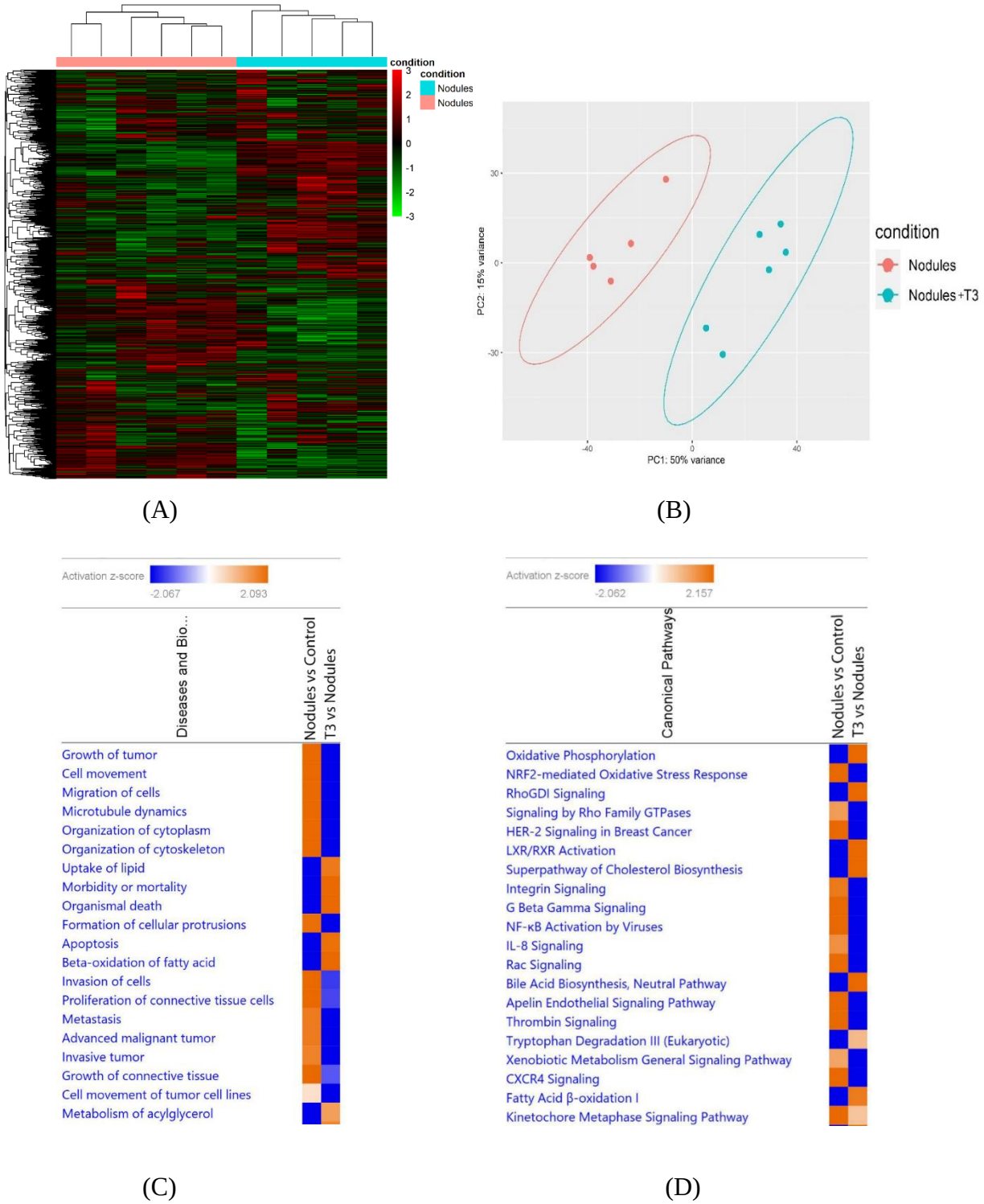

Fig. 16. T3 modifies the global gene expression profile of preneoplastic lesions. **A)** Hierarchical clustering of genes in preneoplastic lesions untreated (nodules), or treated with T3 for 4 days (nodules+T3). Each row represents the expression of a gene and each column a sample. Red and

green colors represent higher or lower mRNA expression levels (median-centered), respectively; **B)** Principal component analysis (PCA) indicative of the variability of gene expression data in nodules of rats untreated or treated with T3 for 4 days; **C)** Top 20 diseases and functions identified by IPA core analysis in untreated nodules vs. control and T3-treated nodules vs. untreated nodules; **D)** Top 20 Canonical Pathways identified by IPA Core Analysis in untreated nodules vs. control and T3-treated nodules vs. untreated nodules. Color is determined by Z-score; the Z-score >2 and <-2 are considered meaningful. Blue color indicates suppressed disease /biological function or canonical pathways; orange indicates activated disease/biological function or canonical pathways.

6.4. Analysis of miRNome in preneoplastic lesions

Study design was organized to allow the comparison of small non-coding RNA and gene expression profiles in the same preneoplastic nodules from rats subjected to a single initiating dose of DEN followed by a promoting procedure (R-H model),(119) and then treated or not with T3 for 4-days . We used NGS to determine the expression of small non-coding RNAs and protein coding genes.

In accordance with previous studies performed with arrays,(43) unsupervised hierarchical cluster analysis stratified control livers and preneoplastic nodules into two clearly defined groups (Fig. 17A). Principal components analysis (PCA) separated the samples according to the two groups (Fig. 17B). Analysis of differentially expressed miRNAs evidenced that 88 miRNAs (cut off 1.4) were modified in their expression, with 49 of them being up-regulated. Notably, 13 among the 15 most down-regulated miRNAs have already been described to act as oncosuppressors in experimental or human HCCs, (120–127) whereas among the differentially up-regulated miRNAs some were similarly regulated in human HCC (miR-181, miR-183-5p, miR-421 and miR-21); (90,128–130) several miRNAs of uncertain function were never described in relation with liver cancer.

MiR-224, the most up-regulated in the nodules (+254 fold vs. controls), was recently shown to target deiodinase 1 (Dio1), an enzyme expressed in liver and kidney and needed for the conversion of T4 to T3, in rat hepatocytes and human renal carcinoma cells. (58,131). Moreover, at least two other miRs found up-regulated - miR-421-3p and miR-185-5p - were also predicted (Target Scan), but not experimentally validated, to target Dio1, further supporting the notion that local hypothyroidism can favour progression to HCC. (41)

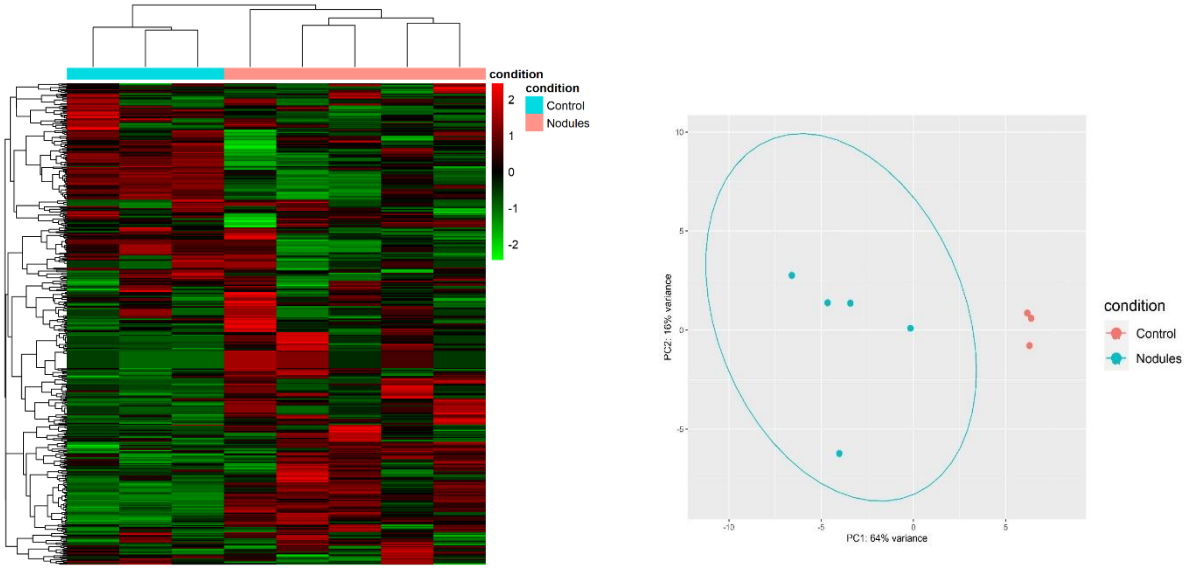

(A) (B)

Fig. 17. **A)** Hierarchical clustering of miRNAs in preneoplastic lesions (nodules), and control samples. Each row represents the expression of a gene and each column a sample. Red and green colors represent higher or lower mRNA expression levels (median-centered), respectively; **B)** PCA of miRNAs in preneoplastic lesions (nodules), and control samples.

6.5. Effect of T3 on microRNA profile of preneoplastic nodules.

MiR NGS analysis was performed in the same nodules analyzed for transcriptomics. Unsupervised hierarchical cluster and PCA analyses stratified the samples into two different clusters, with the exception of two samples (Fig.18 A, B). Analysis of differentially expressed miRNAs identified 28 miRNAs (cut off ≥ 1.4), with 12 of them being up-regulated (Fig.18C). MiRNAs have been reported to act by binding to the promoter region, and to specific sequences in UTR and coding regions. Interaction with the promoter region has been reported to preferentially induce transcription, while binding to the UTR sites and coding sequence to predominantly induce transcriptional repression. (85,132,133) In this study, we only analysed miRNAs binding to the UTR sites.

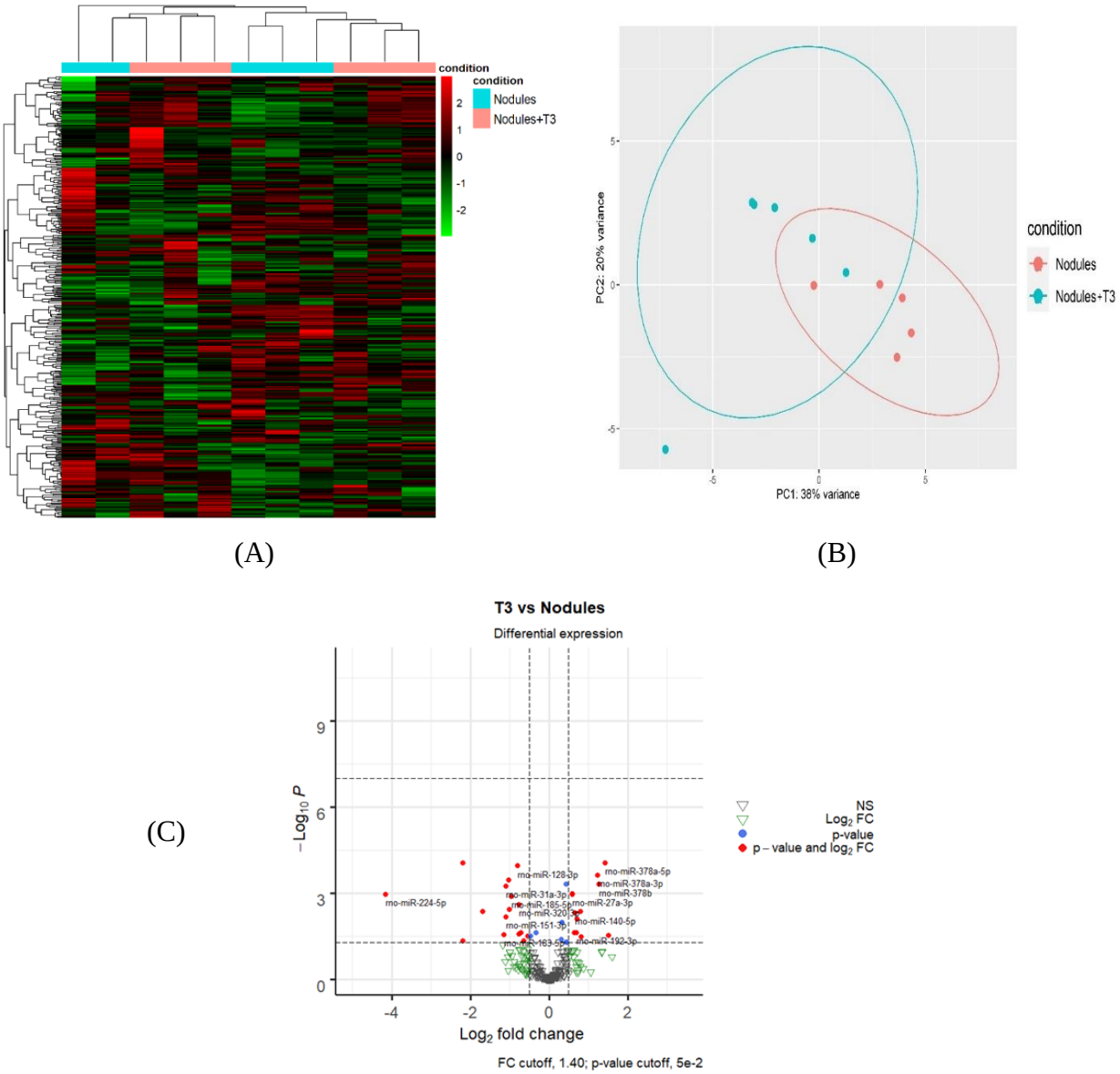

Fig. 18. T3 modifies the global miRNA expression profile of preneoplastic lesions **A)** Hierarchical clustering of miRNA in preneoplastic lesions untreated (nodules), or treated with T3 for 4 days (nodules +T3). Each row represents the expression of a gene and each column a sample. Red and green colors represent higher or lower miRNA expression levels (median-centered), respectively. **B)** Principal component analysis (PCA) indicative of the variability of miRNA expression data in nodules untreated or treated with T3 for 4 days. **C)** Volcano plot of the 28 significantly differentially expressed miRNAs. Red dots indicate the miRNAs which qualify the P-value of 0.05 and FC 1.4. Green and grey triangles indicate miRNAs which did not pass the P-value and Fold change cutoff respectively.

6.6. Integrative Analysis of miRNA-mRNA Expression Profiles.

A state of local hypothyroidism represents a promoting condition for the progression of preneoplastic lesions to HCC, (41) and restoration of a normal T3/Thr axis is associated to their regression. (43,134) However, whether miRs are involved in the increased expression of Thrβ target genes is unclear. Therefore, we also investigated whether relevant changes in miRNAs targeting Thrβ, Dio1 or other genes involved in the activation of the THR/RXR pathway take place after T3. Our analysis showed down-regulation of miR-224 and miR-185-5p, two miRs known (58,131) or predicted (TargetScan) to target Dio1. Notably, miR-224 - which was the most up-regulated in the nodules when compared to controls (254-fold) - was also the most-downregulated following T3 treatment; conversely, transcriptomic analysis performed in the same nodules showed that Dio1 was up-regulated in T3-treated nodules (12-fold increase) compared to untreated nodules. Dio1 up-regulation was also associated with a concomitant decreased expression of miR-182 (-2.01 fold) and miR-185-5p (-1.92 fold). The possible role of miRs in the reversion from a local hypo- to a hyperthyroid state of the nodules was also supported by the finding that miR-425-5p - predicted to target Thrβ – and upregulated in preneoplastic nodules, was down-regulated by T3 treatment in parallel with enhanced TRβ mRNA levels.

No inverse correlation between miRs and TRβ expression was observed for other miRs previously suggested as TRβ regulators, such as miR-155. (135)

6.6.1. Nrf2-Mediated Oxidative Stress Response.

Nrf2 pathway has been previously shown to promote HCC development in humans as well as in experimental models. (136) Accordingly, we investigated whether miRs could be involved in the pathways most modified by T3 treatment, and in particular the Nrf2 and the Oxidative Phosphorylation pathways. Among the miRNAs whose expression was up-regulated by T3 treatment, we found a number of miRs known or predicted to target genes involved in the activation of the Nrf2 pathway. Up-regulation of Nrf2 has been observed in the experimental model herein used and T3 treatment was shown to reverse Nrf2 activation, although the mechanisms underlying this effect were not defined. (137) The present NGS analysis revealed that most Nrf2-target genes were down-regulated by T3 treatment (Fig. 19A), and, interestingly, this effect was associated with up-regulation of 6 miRs predicted (miR-27a, 378a-5p, 532-3p, 802-5p, 672-5p) or shown (miR-140-5p) to target Nrf2 or genes involved in the Keap1-Nrf2 pathway.

(138) It is also worth to mention that the decreased expression G6pd, another Nrf2 target implicated in the metabolic reprogramming of preneoplastic lesions was paralleled with up-regulation of miRNA-672-5p (Fig. 19A).

6.6.2. Oxidative Phosphorylation

Another pathway strongly modified by T3 treatment is the Oxidative Phosphorylation pathway that was down-regulated in preneoplastic nodules (for a comparison see Fig. 19B and 15B). Among the miRs whose expression was down-regulated by T3 treatment, we found 9 miRs predicted to target the five mitochondrial complexes (miR151-3p, 185-5p, 128-3p,182- 5p, 193a-3p, 128-5p, 425-5p, 320-3p, 224-5p). Notably, the induction of miR-182 has also been reported to promote glucose metabolism in non-small lung cancer cells. (139) Thus, the switch from glycolysis to OXPHOS induced by T3 may be mediated, at least in part, by downregulation of this miR.

6.6.3. Proline Biosynthesis Pathway

Together with the switch from glycolysis to OXPHOS, T3 treatment also led to inhibition of proline biosynthesis, recently shown to be required for HCC progression. (140) Indeed, as demonstrated in Fig. 20A, the expression of Pycr1 and Aldh18a1, two enzymes involved in proline synthesis, was up-regulated in nodules and down regulated following treatment with T3. To directly establish whether T3 could affect proline biosynthesis, we analyzed the expression of Pycr1 and Aldh18a1 in Thrβ-transfected HepG2 cells. As shown in Fig. 20B, T3 significantly diminished the expression of both the genes in mock as well as in Thrβ-transfected cells. Notably, among the miRs modified by thyroid hormone was miR-672-5p, predicted to target Pycr1

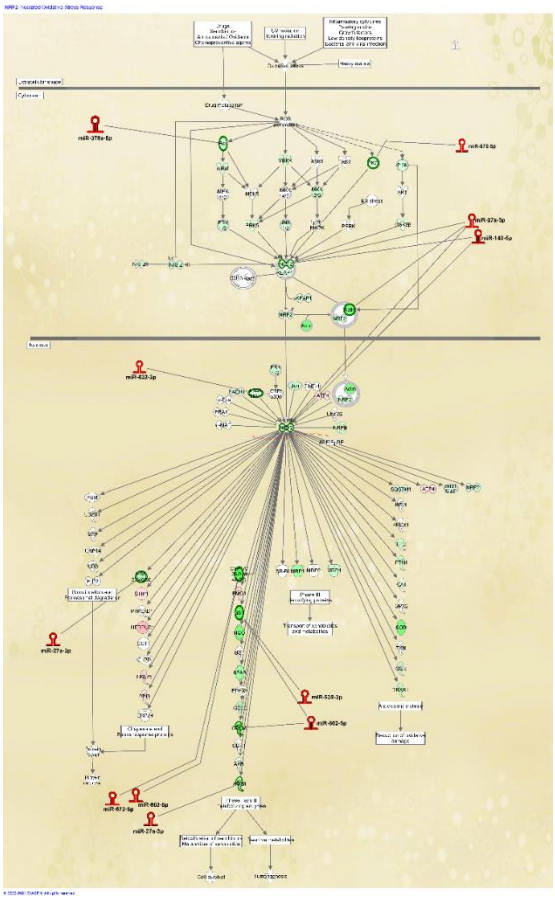

(A)

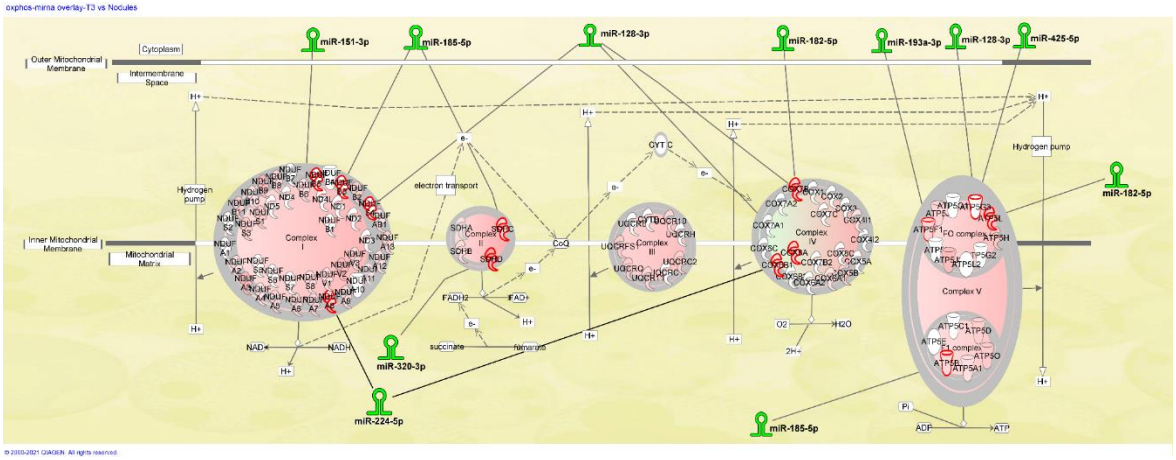

(B)

Fig. 19. MiRNA:mRNA integrated network and proline biosynthesis in preneoplastic nodules following T3 treatment **A)** IPA analysis of Nrf2 oxidative stress response pathway in T3 treated nodules vs. untreated nodules; **B)** IPA analysis of Oxidative Phosphorylation pathway in T3-treated nodules vs. untreated nodules.

Gene	Samples	Fold Change
Pycr1	• Nodules vs. Control • Nodules + T3 vs. Nodules	10.83 -1.62
Aldh18a1	• Nodules vs. Control • Nodules + T3 vs. Nodules	326.68 3.26*
Prodh2	• Nodules vs. Control • Nodules + T3 vs. Nodules	-4.41 1.82

*P-adjusted value > 0.05

(A)

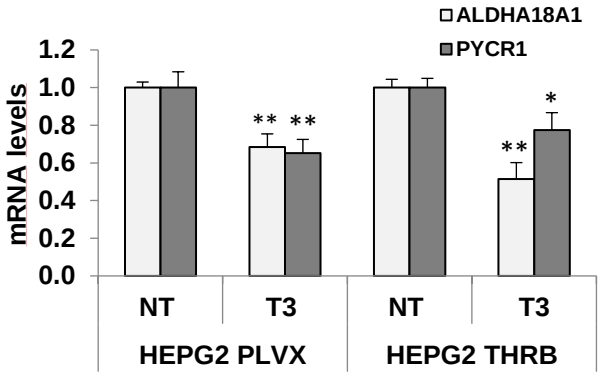

(B)

Fig. 20. A) Results of NGS analysis showing fold change of the key genes involved in proline metabolism: Pycr1, Aldh18a1 and Prodh. P-adjusted value = 0.05 and fold change ± 1.5. **B)** qRT PCR analysis of the expression of PYCR1 and ALDH18a1 in HepG2 cells not transduced (PLVX) or transduced with THRB and treated (T3) or not (NT) for 48 hours with 100nM T3. MiRNA expression was calculated as fold change using the $2^{-\Delta\Delta Ct}$ method and RNU48 as endogenous control. Student t-test: **P*<0.05; ***P*<0.01

6.7. In-vitro validation of selected mRNA and miRNA in HCC

Preneoplastic nodules are considered, as a population, the precursors of HCC. However, it is known that not all the genetic/epigenetic changes found at early stages of hepatocarcinogenesis are maintained until the final steps of this process. (141,142)

To directly establish whether miRs could play a role in the T3-modified molecular pathways in HCC, we analyzed the expression of miRNAs involved in the T3/Thr axis and in the Nrf2 pathway in HepG2 cells transduced with lentiviral vector expressing THRB gene, with and without T3 treatment. As shown in Fig. 21A, differently from what was observed in T3-treated preneoplastic nodules, no change of the expression of miRNAs involved in Keap1-Nrf2 pathway, OXPHOS and T3/Thr axis (miR-140, miR-185, miR-421, miR-425 and miR-224) was detected in mock or Thrβ−transfected HepG2 or Mahlavu cells exposed to thyroid hormone.

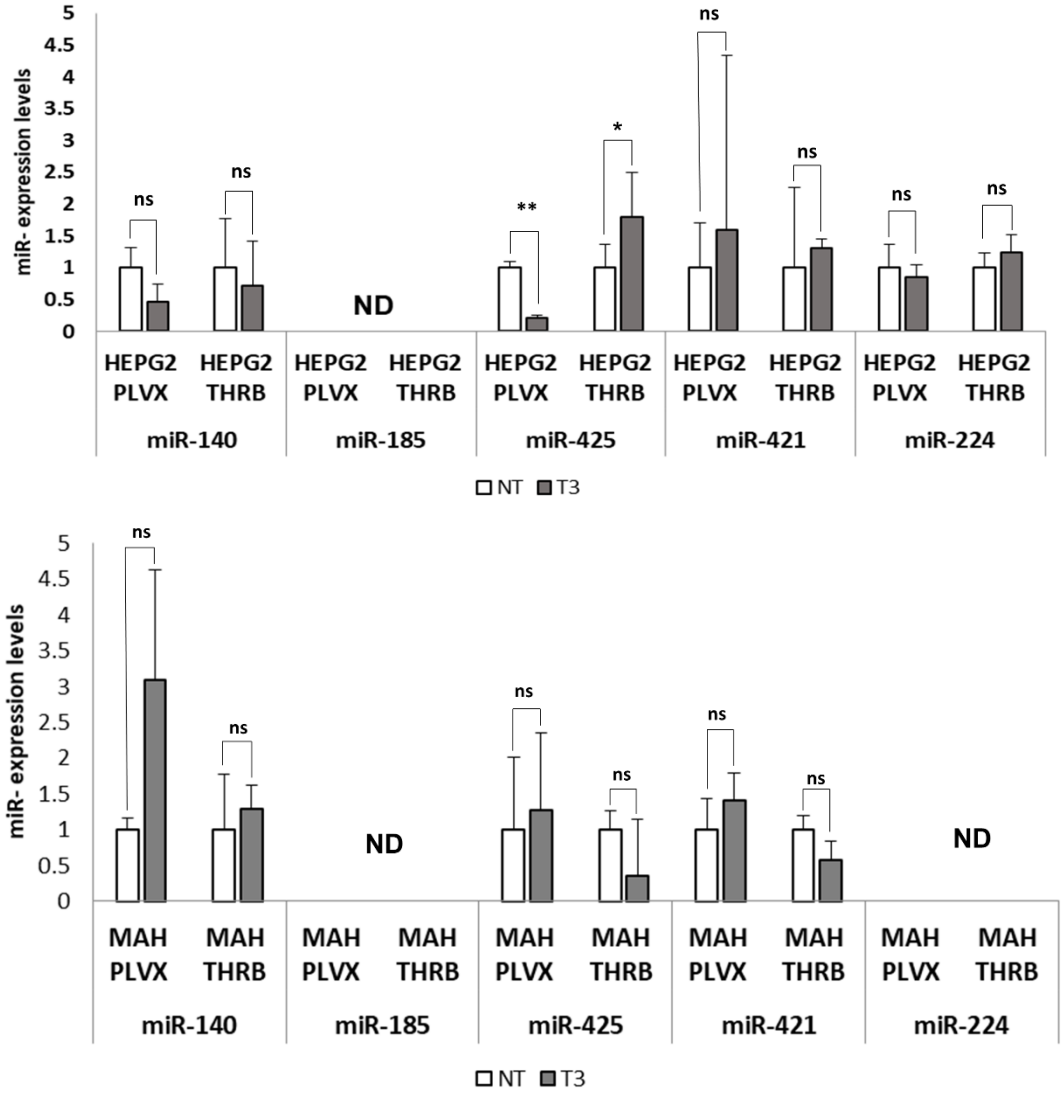

(A)

Fig. 21. **A)** Expression of miR-140, 185, 425 and 421, and 224 in HepG2 or Mahlavu cells transduced with empty vector (PLVX) or with the vector containing the THRB cDNA and treated (T3) or not (NT) for 48 hours with 100nM T3. Each sample was run in triplicate and gene expression analysis of SNU48 was used as endogenous control. Relative quantification analysis for each gene was calculated by $2^{-\Delta\Delta Ct}$ method; ND: not detected; Student t-test: **P*<0.05; ***P*<0.01; ns: non-significant.

To further investigate whether the expression of miRs associated to T3-induced metabolic reprogramming of preneoplastic nodules is affected by T3 also at late stages of hepatocarcinogenesis, we analyzed by qRT-PCR the expression of some of the genes/miRNAs engaged in the T3/Thr axis or in the Nrf2 pathway in laser-microdissected HCCs generated 10 months after DEN in rats exposed or not to T3 treatment (Fig. 8B). The expression of genes implicated in the Keap1-Nrf2 pathways (Fig. 22C, Nqo1, Gstp1), T3/THR axis (Dio1) and of a specific marker of the most aggressive lesions – cytokeratin-19 (Krt-19) – was affected by T3 in a similar manner both in preneoplastic nodules and HCCs (Fig. 22A, 22C). On the contrary all of the examined miRs in pre-neoplastic nodules (miR-224; miR-425; miR185; miR-27) were not modified with the exception of miR-182 (Fig. 22B). These results suggest that the effect of T3 on these pathways in HCC is no longer dependent upon the vast majority of these miRNAs.

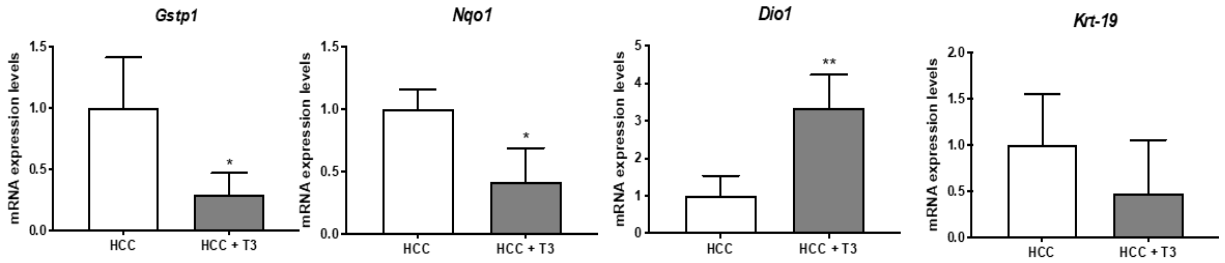

(A)

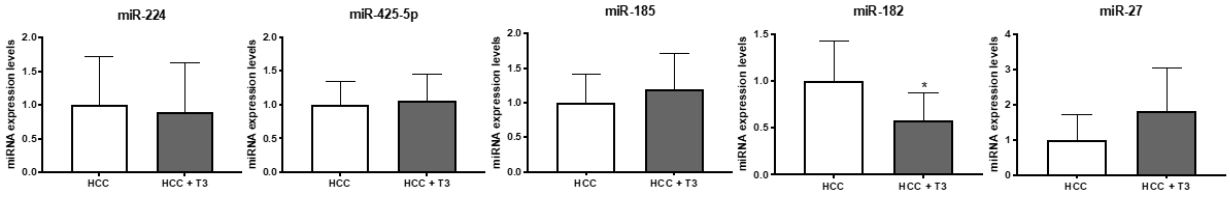

(B)

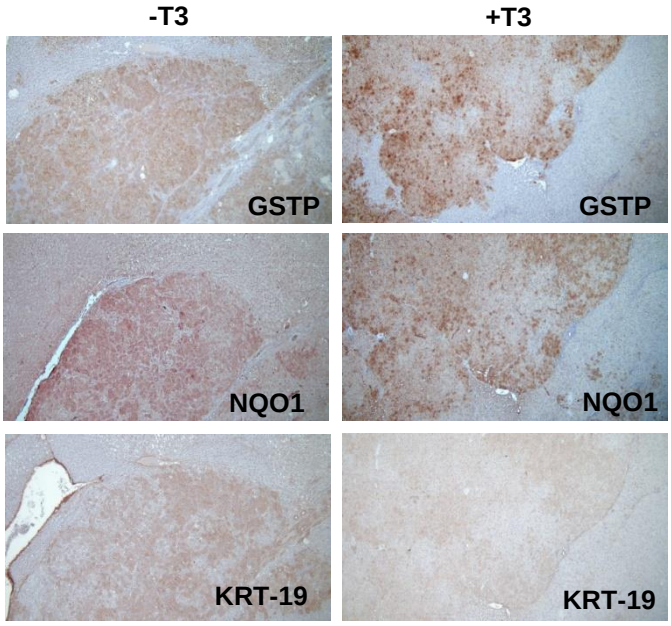

(C)

Fig. 22. A) qRT-PCR analysis of the expression of *Gstp, Nqo1, Dio1* and *Krt-19* in HCC bearing rats. Rats exposed to the R-H protocol were sacrificed 10 months after treatment with a single dose of DEN. The week prior to sacrifice, one group of animals was fed a T3-supplemented diet as described in Materials and Methods. Each sample was run in triplicate and gene expression analysis of beta-actin was used as endogenous control. Relative quantification analysis for each gene was calculated by $2^{-\Delta\Delta Ct}$ method. Student t-test: **P*<0.05; ***P*<0.01; (X5); **B)** qRT-PCR analysis of the expression of miR-224, miR-425-5p, miR-185, miR-182, and miR-27 in HCC bearing rats. Rats were treated as described B. Each sample was run in triplicate and gene expression analysis of *Gapdh* was used as endogenous control. Relative quantification analysis for each gene was calculated by $2^{-\Delta\Delta Ct}$ method. Student t-test: **P*<0.05. **C)** GSTP, NQO1 and KRT-19 immunohistochemistry of HCCs from livers of animals treated as described in Fig 8B.

7. DISCUSSION

MicroRNAs are a large family of endogenous, small-non coding RNAs that function post-transcriptionally in the regulation of gene expression. As far as HCC is concerned, miRNAs have increasingly gained importance due to their widespread occurrence and diverse functions as regulatory molecules in all aspects of cancer biology, such as proliferation, invasion, apoptosis, and angiogenesis. Importantly, miRNAs appear to play a critical role not only in HCC but also at the initial steps of hepatocarcinogenesis in both experimental and human studies. (143)

Previous studies have reported the anti-tumorigenic effect of T3 on rat hepatic preneoplastic nodules (134). The effect of T3 and the reprogramming of poorly differentiated hepatocytes to a more mature phenotype that causes the disappearance of preneoplastic nodules is not fully understood. In this study, we utilized NGS to carry out an in-depth analysis of miRNAs and mRNAs in preneoplastic nodules following T3 treatment. The present work unveiled dysregulated pathways and their miRNA-mRNA pairs involved in the regression of preneoplastic nodules. We identified 28 differentially expressed miRNAs in T3 treated nodules compared to preneoplastic lesions not exposed to thyroid hormone. Among the major pathways that were significantly dysregulated there were Oxidative Phosphorylation, and NRF2 mediated oxidative stress response. Down-regulation of OXPHOS and subsequent activation of glycolysis are well established in proliferating liver cancer cells as they dramatically reprogram some of the metabolic pathways to meet the increased energetic and anabolic needs. T3 treatment for 4 days caused down-regulation of 8 miRNAs predicted/shown to target genes of membrane mitochondrial complexes. Down-regulation of these miRNAs was associated with the up-regulation of 90% of the genes involved in the mitochondrial respiratory chain and to the restoration of OXPHOS. Among the down-regulated miRNAs, 5 have been reported to act as OncomiRNAs in HCC; indeed, miR-224, miR-425, miR-151-3p, miR-182-5p, and have been shown to promote cell proliferation, invasion, and metastasis. (144–147)

Interestingly, miR-224, which is predicted to target Ubiquinone Oxidoreductase Subunit A8 and Cytochrome c oxidase subunit 6B1, has been reported as an early-stage biomarker in HCC patients (148). Recently, it has also been established that it accelerates HCC progression. (149) We also observed up-regulation of the Succinate dehydrogenase complex, a tetramer consisting of SDHA, SDHB, SDHC, and SDHD subunits. Succinate dehydrogenase has a critical tumor-

suppressive role and has been suggested as an important drug target in HCC. 53 Mir-185-5p and mir-320-3p, which are predicted to target of Succinate Dehydrogenase Complex Subunit C (SDHC) and Succinate Dehydrogenase Complex Subunit D (SDHD) respectively, were down-regulated in T3 treated nodules. Additionally, up-regulation of miR-320-3p has also been implicated in early stages of steatohepatitis, a condition favoring HCC development. (150)

Cancer cell proliferation leads to the accumulation of reactive oxygen species (ROS). Cellular oxidants activate the Nrf2 signaling pathway that protects cancer cells from DNA damage. T3 treatment significantly down-regulated this pathway in preneoplastic nodules, as documented by the up-regulation of 6 miRNAs predicted/shown to target genes involved in this pathway. Interestingly, 3 of these miRs exhibited a tumor-suppressive role during HCC progression. MiR 378a-3p, which is predicted to target RAS Like Proto-Oncogene B, has a protective role in liver fibrosis by inactivating hepatic stellate cells, (151,152) whereas miR 27a-3p and 140-5p - predicted to target NRF2 - inhibit cell viability and migration in HCC. (153,154) The present study also confirms that T3 is able to revert the local hypothyroid status of preneoplastic and neoplastic hepatocytes and suggests that some miRNAs (i.e. miR-224 and miR-185-5p) may play a role in restoring the thyroid status, at least at the early stages of tumorigenesis.

Metabolic alterations in cancer are mainly focused on aerobic glycolysis and central carbon metabolism, including the citric acid cycle and the pentose phosphate pathway. Nevertheless, several reports suggested that amino acids may also play a relevant role to support survival and proliferation of cancer cells. (155) In this context, recent studies demonstrated that proline biosynthesis by modulating the expression of the enzymes involved in the biosynthetic process, significantly influences proliferation of HCC cell lines in vitro and tumor formation in vivo. (140) Our NGS analysis enabled us to show that T3, in addition to a switch from glycolysis to OXPHOS, profoundly modifies proline biosynthesis by inhibiting on 18 the one hand the expression of the two enzymes critically involved in proline formation and, on the other hand, up-regulating Prodh which is involved in proline catabolism. Of note, these effects were observed in both preneoplastic nodules as well as in HCCs and HepG2-Thrβ transfected cells. Altogether, these results provide novel information on the anti-tumorigenic role of T3, suggesting the thyroid hormone as a critical player in interfering with metabolic pathways altered in HCC development. Furthermore, intercrossing miRNAs-mRNAs revealed that T3- induced regression of preneoplastic nodules is

accompanied by deregulation of a number of miRNAs that target genes involved in metabolic pathways altered at early stages of HCC development; however, our data also point out that the miRNAs found dysregulated at early stages are unlikely involved at the final steps of tumorigenesis. Whether other miRNAs yet to be defined are implicated in the metabolic switch associated to T3-induced regression of HCC remains to be established.

8. CONCLUSIONS

The present study showed that: i) a number of miRNAs modified by T3 are likely associated to T3-induced regression of preneoplastic nodules; ii) the anti-tumorigenic effect of T3 is mediated by miRNAs implicated in reverting metabolic pathways altered in cancer; iii) proline biosynthesis, up-regulated in HCC, is profoundly inhibited by T3 at both early and late stages. These results are relevant as they can help in the development of novel strategies based on the use of novel thyromimetics, devoid of T3-induced adverse side effects, as therapeutic cancer drugs in the treatment of early stages of human HCC development.

We have also implemented two computational analysis workflows. RIDE and SRIDE are easy-to-manage RNA-Seq and small RNA-Seq analysis workflows. Both the pipeline includes complete workflow, starting with QC of the raw FASTQ files, going through optional trimming, alignment, and counting.

Running these workflows requires a moderate knowledge of programming skills, however, well-written tutorials help the users to set up and run the workflows from scratch. RIDE and SRIDE can be applied to raw FASTQ reads from any organism, where users can provide the reference genome and transcriptome downloaded from UCSC and Ensembl genome browser respectively.

RIDE and SRIDE are built on the basis of Conda and Snakemake, thus making installation and management very easy. All the required tools are available on the Anaconda cloud (https://anaconda.org/) and are wrapped in a virtual environment managed by Conda, making both the workflows independent of the underlying system thus avoiding package/library version conflicts. Both the workflows are defined by rules managed by Snakemake, making them highly modular. Advanced users can easily extract parts of the workflow or expand it based on their own research needs, and replace the tools used in RIDE and SRIDE with other tools to explore new pipelines for analyzing RNA-Seq and small RNA-Seq data.

9. REFERENCES

1. Bray F, Ferlay J, Soerjomataram I, Siegel RL, Torre LA, Jemal A. Global cancer statistics 2018: GLOBOCAN estimates of incidence and mortality worldwide for 36 cancers in 185 countries. CA Cancer J Clin. 2018 Nov;68(6):394–424.
2. Philips CA, Rajesh S, Nair DC, Ahamed R, Abduljaleel JK, Augustine P. Hepatocellular Carcinoma in 2021: An Exhaustive Update. 2021;
3. McGlynn KA, Petrick JL, London WT. Global epidemiology of hepatocellular carcinoma: an emphasis on demographic and regional variability. Clin Liver Dis. 2015 May;19(2):223–38.
4. Parikh S, Hyman D. Hepatocellular Cancer: A Guide for the Internist. Am J Med. 2007;120(3):194–202.
5. Hepatocellular carcinoma T-RS. Epidemiology, risk factors and pathogenesis. World J Gastroenterol. 2008;14(27).
6. No Title. p. https://www.who.int/news-room/fact-sheets/detail/h.
7. Levrero M, Zucman-Rossi J. Mechanisms of HBV-induced hepatocellular carcinoma. J Hepatol [Internet]. 2016;64(1):S84–101. Available from: http://dx.doi.org/10.1016/j.jhep.2016.02.021
8. Tang LSY, Covert E, Wilson E, Kottilil S. Chronic Hepatitis B Infection A Review. 2018; Available from: https://jamanetwork.com/
9. Sandhu HS, Roesel S, Sharifuzzaman M, Chunsuttiwat S TR. Progress Toward Hepatitis B Control — South-East Asia Region, 2016–2019.
10. Lin CL, Kao JH. Prevention of hepatitis b virus-related hepatocellular carcinoma. Hepatoma Res. 2021;7.
11. Hepatitis C. Available from: https://www.who.int/news-room/fact-sheets/detail/hepatitis-c
12. Llovet JM, Zucman-Rossi J, Pikarsky E, Sangro B, Schwartz M, Sherman M, et al. Hepatocellular carcinoma. Nat Rev Dis Prim. 2016 Apr;2:16018.
13. Asselah T, Boyer N, Saadoun D, Martinot-Peignoux M, Marcellin P. Direct-acting antivirals for the treatment of hepatitis C virus infection: optimizing current IFN-free treatment and future perspectives. 2015;
14. Younossi ZM, Koenig AB, Abdelatif D, Fazel Y, Henry L, Wymer M. Global Epidemiology of Nonalcoholic Fatty Liver Disease-Meta-Analytic Assessment of Prevalence, Incidence, and Outcomes. 2015; Available from: http://www.prisma-statement.org/
15. Regimbeau JM, Colombat M, Mognol P, Durand F, Abdalla E, Degott C, et al. Obesity and Diabetes as a Risk Factor for Hepatocellular Carcinoma. 2004; Available from: www.interscience.wiley.com
16. Polesel J, Zucchetto A, Montella M, Dal Maso L, Crispo A, La Vecchia C, et al. The

impact of obesity and diabetes mellitus on the risk of hepatocellular carcinoma. Ann Oncol [Internet]. 2009;20(2):353–7. Available from: https://doi.org/10.1093/annonc/mdn565

17. Pennisi G, Celsa C, Giammanco A, Spatola F, Petta S. Molecular Sciences The Burden of Hepatocellular Carcinoma in Non-Alcoholic Fatty Liver Disease: Screening Issue and Future Perspectives. Available from: www.mdpi.com/journal/ijms

18. Lange NF, Radu P, Dufour JF. Prevention of NAFLD-associated HCC: Role of lifestyle and chemoprevention. J Hepatol [Internet]. 2021;75(5):1217–27. Available from: https://doi.org/10.1016/j.jhep.2021.07.025

19. Matsushita H, Takaki A. Alcohol and hepatocellular carcinoma. Available from: http://bmjopengastro.bmj.com/

20. Organization WH. Global status report on alcohol and health, 2014. 2014;

21. Jepsen, P., Ott, P., Andersen, P. K., Sørensen HT, & Vilstrup H. Risk for hepatocellular carcinoma in patients with alcoholic cirrhosis. Ann Intern Med. 2012;

22. Morgan TR, Mandayam S, Jamal MM. Alcohol and hepatocellular carcinoma. Gastroenterology. 2004;127(5 SUPPL.):87–96.

23. Rich NE, Yopp AC, Singal AG, Murphy CC. Hepatocellular Carcinoma Incidence is Decreasing Among Younger Adults in the United States. Clin Gastroenterol Hepatol [Internet]. 2020 Jan 1 [cited 2022 Jan 17];18(1):242. Available from: /pmc/articles/PMC6817412/

24. Rich NE, Hester C, Odewole M, Murphy CC, Parikh ND, Marrero JA, et al. Racial and Ethnic Differences in Presentation and Outcomes of Hepatocellular Carcinoma. Clin Gastroenterol Hepatol [Internet]. 2019 Feb 1 [cited 2022 Jan 17];17(3):551. Available from: /pmc/articles/PMC6274621/

25. Chen K, Chang P-E, Goh GB-B, Tan C-K. Surveillance for hepatocellular carcinoma - current status and advances. Hepatoma Res [Internet]. 2018 Dec 12 [cited 2022 Jan 17];4:72. Available from: https://hrjournal.net/article/view/2920

26. Galle PR, Forner A, Llovet JM, Mazzaferro V, Piscaglia F, Raoul JL, et al. EASL Clinical Practice Guidelines: Management of hepatocellular carcinoma. J Hepatol [Internet]. 2018 Jul 1 [cited 2022 Jan 17];69(1):182–236. Available from: https://pubmed.ncbi.nlm.nih.gov/29628281/

27. Llovet JM, Villanueva A, Marrero JA, Schwartz M, Meyer T, Galle PR, et al. Trial Design and Endpoints in Hepatocellular Carcinoma: AASLD Consensus Conference. Hepatology [Internet]. 2021 Jan 1 [cited 2022 Jan 17];73 Suppl 1(S1):158–91. Available from: https://pubmed.ncbi.nlm.nih.gov/32430997/

28. Llovet JM, Brú C, Bruix J. Prognosis of hepatocellular carcinoma: the BCLC staging classification. Semin Liver Dis [Internet]. 1999 [cited 2022 Jan 17];19(3):329–37. Available from: https://pubmed.ncbi.nlm.nih.gov/10518312/

29. Cheng AL, Kang YK, Chen Z, Tsao CJ, Qin S, Kim JS, et al. Efficacy and safety of

sorafenib in patients in the Asia-Pacific region with advanced hepatocellular carcinoma: a phase III randomised, double-blind, placebo-controlled trial. Lancet Oncol [Internet]. 2009 Jan [cited 2022 Jan 17];10(1):25–34. Available from: https://pubmed.ncbi.nlm.nih.gov/19095497/

30. Zhou J, Sun HC, Wang Z, Cong WM, Wang JH, Zeng MS, et al. Guidelines for Diagnosis and Treatment of Primary Liver Cancer in China (2017 Edition). Liver cancer [Internet]. 2018 Sep 1 [cited 2022 Jan 17];7(3):235–60. Available from: https://pubmed.ncbi.nlm.nih.gov/30319983/

31. Park JW, Lee JS, Suh KS, Chung JW, Seong J, Kim DY, et al. 2018 Korean Liver Cancer Association-National Cancer Center Korea Practice Guidelines for the Management of Hepatocellular Carcinoma. Gut Liver [Internet]. 2019 [cited 2022 Jan 17];13(3):227–99. Available from: https://pubmed.ncbi.nlm.nih.gov/31060120/

32. Qin S, Bi F, Gu S, Bai Y, Chen Z, Wang Z, et al. Donafenib Versus Sorafenib in First-Line Treatment of Unresectable or Metastatic Hepatocellular Carcinoma: A Randomized, Open-Label, Parallel-Controlled Phase II-III Trial. J Clin Oncol [Internet]. 2021 Sep 20 [cited 2022 Jan 17];39(27):3002–11. Available from: https://pubmed.ncbi.nlm.nih.gov/34185551/

33. Marino D, Zichi C, Audisio M, Sperti E, Di Maio M. Second-line treatment options in hepatocellular carcinoma. Drugs Context [Internet]. 2019 [cited 2022 Jan 17];8:212577. Available from: /pmc/articles/PMC6469745/

34. Pathak S, Sonbol MB. Second-Line Treatment Options for Hepatocellular Carcinoma: Current Landscape and Future Direction . J Hepatocell Carcinoma [Internet]. 2021 Sep 21 [cited 2022 Jan 17];8:1147–58. Available from: https://www.dovepress.com/second-line-treatment-options-for-hepatocellular-carcinoma-current-lan-peer-reviewed-fulltext-article-JHC

35. Huang A, Yang XR, Chung WY, Dennison AR, Zhou J. Targeted therapy for hepatocellular carcinoma. Signal Transduct Target Ther [Internet]. 2020 Dec 1 [cited 2022 Jan 17];5(1). Available from: /pmc/articles/PMC7419547/

36. Onuma AE, Zhang H, Huang H, Williams TM, Noonan A, Tsung A. Immune Checkpoint Inhibitors in Hepatocellular Cancer: Current Understanding on Mechanisms of Resistance and Biomarkers of Response to Treatment. Gene Expr [Internet]. 2020 [cited 2022 Jan 18];20(1):53–65. Available from: https://pubmed.ncbi.nlm.nih.gov/32340652/

37. Hassan MM, Kaseb A, Li D, Patt YZ, Vaunthey JN, Thomas MB, et al. Association Between Hypothyroidism and Hepatocellular Carcinoma: A Case-Control Study in the United States. Hepatology [Internet]. 2009 May [cited 2022 Jan 18];49(5):1563. Available from: /pmc/articles/PMC3715879/

38. Reddy A, Dash C, Leerapun A, Mettler TA, Stadheim LM, Lazaridis KN, et al. Hypothyroidism: A Possible Risk Factor for Liver Cancer in Patients With No Known Underlying Cause of Liver Disease. Clin Gastroenterol Hepatol [Internet]. 2007 Jan 1 [cited 2022 Jan 18];5(1):118–23. Available from: http://www.cghjournal.org/article/S1542356506007683/fulltext

39. Krause C, Grohs M, El Gammal AT, Wolter S, Lehnert H, Mann O, et al. Reduced expression of thyroid hormone receptor β in human nonalcoholic steatohepatitis. Endocr Connect. 2018 Dec;7(12):1448–56.

40. Liao C-H, Yeh C-T, Huang Y-H, Wu S-M, Chi H-C, Tsai M-M, et al. Dickkopf 4 positively regulated by the thyroid hormone receptor suppresses cell invasion in human hepatoma cells. Hepatology. 2012 Mar;55(3):910–20.

41. Frau C, Loi R, Petrelli A, Perra A, Menegon S, Kowalik MA, et al. Local hypothyroidism favors the progression of preneoplastic lesions to hepatocellular carcinoma in rats. Hepatology. 2015 Jan;61(1):249—259.

42. Martínez-Iglesias O, Olmeda D, Alonso-Merino E, Gómez-Rey S, González-López AM, Luengo E, et al. The nuclear corepressor 1 and the thyroid hormone receptor β suppress breast tumor lymphangiogenesis. Oncotarget. 2016 Nov;7(48):78971–84.

43. Kowalik MA, Puliga E, Cabras L, Sulas P, Petrelli A, Perra A, et al. Thyroid hormone inhibits hepatocellular carcinoma progression via induction of differentiation and metabolic reprogramming. J Hepatol. 2020 Jun;72(6):1159–69.

44. Chi H-C, Chen S-L, Tsai C-Y, Chuang W-Y, Huang Y-H, Tsai M-M, et al. Thyroid hormone suppresses hepatocarcinogenesis via DAPK2 and SQSTM1-dependent selective autophagy. Autophagy. 2016 Dec;12(12):2271–85.

45. Chi H-C, Chen S-L, Lin S-L, Tsai C-Y, Chuang W-Y, Lin Y-H, et al. Thyroid hormone protects hepatocytes from HBx-induced carcinogenesis by enhancing mitochondrial turnover. Oncogene. 2017 Sep;36(37):5274–84.

46. Bianco AC, Salvatore D, Gereben B, Berry MJ, Larsen PR. Biochemistry, cellular and molecular biology, and physiological roles of the iodothyronine selenodeiodinases. Endocr Rev [Internet]. 2002 [cited 2022 Jan 18];23(1):38–89. Available from: https://pubmed.ncbi.nlm.nih.gov/11844744/

47. Intracellular Pathways of Iodothyronine Metabolism/Implications of Deiodination for Thyroid Hormone Action | Oncohema Key [Internet]. [cited 2022 Jan 18]. Available from: https://oncohemakey.com/intracellular-pathways-of-iodothyronine-metabolismimplications-of-deiodination-for-thyroid-hormone-action/

48. Davis PJ, Goglia F, Leonard JL. Nongenomic actions of thyroid hormone. Nat Rev Endocrinol. 2016 Feb;12(2):111–21.

49. Lazar MA. Thyroid hormone receptors: multiple forms, multiple possibilities. Endocr Rev. 1993 Apr;14(2):184–93.

50. Brent GA. The molecular basis of thyroid hormone action. N Engl J Med. 1994 Sep;331(13):847–53.

51. Bradley DJ, Towle HC, Young WS. Spatial and temporal expression of alpha- and beta-thyroid hormone receptor mRNAs, including the beta 2-subtype, in the developing mammalian nervous system. J Neurosci [Internet]. 1992 [cited 2022 Jan 18];12(6):2288–302. Available from: https://pubmed.ncbi.nlm.nih.gov/1607941/

52. Cheng SY, Leonard JL, Davis PJ. Molecular aspects of thyroid hormone actions. Endocr Rev [Internet]. 2010 Apr [cited 2022 Jan 18];31(2):139–70. Available from: https://pubmed.ncbi.nlm.nih.gov/20051527/

53. Brent GA. Tissue-specific actions of thyroid hormone: insights from animal models. Rev Endocr Metab Disord. 2000 Jan;1(1–2):27–33.

54. Forrest D, Vennström B. Functions of thyroid hormone receptors in mice. Thyroid. 2000 Jan;10(1):41–52.

55. Dunwell TL, Hesson LB, Pavlova T, Zabarovska V, Kashuba V, Catchpoole D, et al. Epigenetic analysis of childhood acute lymphoblastic leukemia. Epigenetics [Internet]. 2009 Apr 1 [cited 2022 Jan 27];4(3):185–93. Available from: https://pubmed.ncbi.nlm.nih.gov/19430199/

56. Joseph B, Ji M, Liu D, Hou P, Xing MM. Lack of mutations in the thyroid hormone receptor (TR) alpha and beta genes but frequent hypermethylation of the TRbeta gene in differentiated thyroid tumors. J Clin Endocrinol Metab [Internet]. 2007 [cited 2022 Jan 27];92(12):4766–70. Available from: https://pubmed.ncbi.nlm.nih.gov/17911173/

57. Ling Y, Xu X, Hao J, Ling X, Du X, Liu X, et al. Aberrant methylation of the THRB gene in tissue and plasma of breast cancer patients. Cancer Genet Cytogenet [Internet]. 2010 Jan 15 [cited 2022 Jan 27];196(2):140–5. Available from: https://pubmed.ncbi.nlm.nih.gov/20082849/

58. Boguslawska J, Wojcicka A, Piekielko-Witkowska A, Master A, Nauman A. MiR-224 targets the 3'UTR of type 1 5'-iodothyronine deiodinase possibly contributing to tissue hypothyroidism in renal cancer. PLoS One. 2011;6(9):e24541.

59. Boguslawska J, Piekielko-Witkowska A, Wojcicka A, Kedzierska H, Poplawski P, Nauman A. Regulatory feedback loop between T3 and microRNAs in renal cancer. Mol Cell Endocrinol [Internet]. 2014 Mar 25 [cited 2022 Jan 19];384(1–2):61–70. Available from: https://pubmed.ncbi.nlm.nih.gov/24440748/

60. Janssen R, Zuidwijk MJ, Muller A, van Mil A, Dirkx E, Oudejans CBM, et al. MicroRNA 214 is a potential regulator of thyroid hormone levels in the mouse heart following myocardial infarction, by targeting the thyroid-hormone-inactivating enzyme deiodinase type III. Front Endocrinol (Lausanne). 2016 Mar 9;7(MAR):22.

61. Janssen R, Muller A, Simonides WS. Cardiac Thyroid Hormone Metabolism and Heart Failure. Eur Thyroid J [Internet]. 2017 [cited 2022 Jan 19];6(3):130–7. Available from: https://pubmed.ncbi.nlm.nih.gov/28785539/

62. Di Girolamo D, Ambrosio R, De Stefano MA, Mancino G, Porcelli T, Luongo C, et al. Reciprocal interplay between thyroid hormone and microRNA-21 regulates hedgehog pathway-driven skin tumorigenesis. J Clin Invest [Internet]. 2016 Jun 1 [cited 2022 Jan 19];126(6):2308–20. Available from: https://pubmed.ncbi.nlm.nih.gov/27159391/

63. Jazdzewski K, Boguslawska J, Jendrzejewski J, Liyanarachchi S, Pachucki J, Wardyn KA, et al. Thyroid hormone receptor beta (THRB) is a major target gene for microRNAs deregulated in papillary thyroid carcinoma (PTC). J Clin Endocrinol Metab. 2011

Mar;96(3):E546-53.

64. Master A, Wójcicka A, Piekiełko-Witkowska A, Bogusławska J, Popławski P, Tański Z, et al. Untranslated regions of thyroid hormone receptor beta 1 mRNA are impaired in human clear cell renal cell carcinoma. Biochim Biophys Acta. 2010 Nov;1802(11):995–1005.

65. Nishi H, Ono K, Horie T, Nagao K, Kinoshita M, Kuwabara Y, et al. MicroRNA-27a regulates beta cardiac myosin heavy chain gene expression by targeting thyroid hormone receptor beta1 in neonatal rat ventricular myocytes. Mol Cell Biol. 2011 Feb;31(4):744—755.

66. Ruiz-Llorente L, Ardila-González S, Fanjul LF, Martínez-Iglesias O, Aranda A. microRNAs 424 and 503 are mediators of the anti-proliferative and anti-invasive action of the thyroid hormone receptor beta. Oncotarget. 2014 May;5(10):2918–33.

67. Aranda A. MicroRNAs and thyroid hormone action. Mol Cell Endocrinol. 2021 Apr 5;525:111175.

68. Lee RC, Feinbaum RL, Ambros V. The C. elegans heterochronic gene lin-4 encodes small RNAs with antisense complementarity to lin-14. Cell. 1993 Dec 3;75(5):843–54.

69. Sayed D, Abdellatif M. Microrna in development and disease. Physiol Rev [Internet]. 2011 Jul [cited 2022 Jan 18];91(3):827–87. Available from: https://journals.physiology.org/doi/abs/10.1152/physrev.00006.2010

70. Bucur O. microRNA regulators of apoptosis in cancer. Discoveries [Internet]. 2016 Apr 1 [cited 2022 Jan 18];4(1):e57. Available from: /pmc/articles/PMC7159826/

71. Shah MY, Calin GA. MicroRNAs as therapeutic targets in human cancers. Wiley Interdiscip Rev RNA [Internet]. 2014 [cited 2022 Jan 18];5(4):537. Available from: /pmc/articles/PMC4461221/

72. Lee Y, Kim M, Han J, Yeom KH, Lee S, Baek SH, et al. MicroRNA genes are transcribed by RNA polymerase II. EMBO J [Internet]. 2004 Oct 13 [cited 2022 Jan 18];23(20):4051–60. Available from: https://pubmed.ncbi.nlm.nih.gov/15372072/

73. Bortolin-Cavaille ML, Dance M, Weber M, Cavaille J. C19MC microRNAs are processed from introns of large Pol-II, non-protein-coding transcripts. Nucleic Acids Res [Internet]. 2009 [cited 2022 Jan 18];37(10):3464–73. Available from: https://pubmed.ncbi.nlm.nih.gov/19339516/

74. Denli AM, Tops BBJ, Plasterk RHA, Ketting RF, Hannon GJ. Processing of primary microRNAs by the Microprocessor complex. Nat 2004 4327014 [Internet]. 2004 Nov 7 [cited 2022 Jan 19];432(7014):231–5. Available from: https://www.nature.com/articles/nature03049

75. Gregory RI, Yan KP, Amuthan G, Chendrimada T, Doratotaj B, Cooch N, et al. The Microprocessor complex mediates the genesis of microRNAs. Nature [Internet]. 2004 Nov 11 [cited 2022 Jan 19];432(7014):235–40. Available from: https://pubmed.ncbi.nlm.nih.gov/15531877/

76. Llovet JM, Ricci S, Mazzaferro V, Hilgard P, Gane E, Blanc J-F, et al. Sorafenib in advanced hepatocellular carcinoma. N Engl J Med [Internet]. 2008 Jul 24 [cited 2022 Jan 17];359(4):378–90. Available from: https://pubmed.ncbi.nlm.nih.gov/18650514/

77. Han J, Lee Y, Yeom KH, Kim YK, Jin H, Kim VN. The Drosha-DGCR8 complex in primary microRNA processing. Genes Dev [Internet]. 2004 Dec 15 [cited 2022 Jan 19];18(24):3016–27. Available from: https://pubmed.ncbi.nlm.nih.gov/15574589/

78. Lund E, Güttinger S, Calado A, Dahlberg JE, Kutay U. Nuclear export of microRNA precursors. Science [Internet]. 2004 Jan 2 [cited 2022 Jan 19];303(5654):95–8. Available from: https://pubmed.ncbi.nlm.nih.gov/14631048/

79. Bohnsack MT, Czaplinski K, Görlich D. Exportin 5 is a RanGTP-dependent dsRNA-binding protein that mediates nuclear export of pre-miRNAs. RNA [Internet]. 2004 Feb [cited 2022 Jan 19];10(2):185–91. Available from: https://pubmed.ncbi.nlm.nih.gov/14730017/

80. Yi R, Qin Y, Macara IG, Cullen BR. Exportin-5 mediates the nuclear export of pre-microRNAs and short hairpin RNAs. Genes Dev [Internet]. 2003 Dec 15 [cited 2022 Jan 19];17(24):3011–6. Available from: https://pubmed.ncbi.nlm.nih.gov/14681208/

81. Sontheimer EJ. Assembly and function of RNA silencing complexes. Nat Rev Mol Cell Biol 2005 62 [Internet]. 2005 Jan 14 [cited 2022 Jan 19];6(2):127–38. Available from: https://www.nature.com/articles/nrm1568

82. Cai X, Hagedorn CH, Cullen BR. Human microRNAs are processed from capped, polyadenylated transcripts that can also function as mRNAs. RNA [Internet]. 2004 Dec [cited 2022 Jan 19];10(12):1957–66. Available from: https://pubmed.ncbi.nlm.nih.gov/15525708/

83. Peng Y, Croce CM. The role of MicroRNAs in human cancer. Signal Transduct Target Ther 2016 11 [Internet]. 2016 Jan 28 [cited 2022 Jan 19];1(1):1–9. Available from: https://www.nature.com/articles/sigtrans20154

84. Hsu S hao, Ghoshal K. MicroRNAs in Liver Health and Disease. Curr Pathobiol Rep [Internet]. 2013 Mar 1 [cited 2022 Jan 19];1(1):53. Available from: /pmc/articles/PMC3616382/

85. Lujambio A, Lowe SW. The microcosmos of cancer. Nature. 2012 Feb;482(7385):347–55.

86. Datta J, Kutay H, Nasser MW, Nuovo GJ, Wang B, Majumder S, et al. Methylation mediated silencing of MicroRNA-1 gene and its role in hepatocellular carcinogenesis. Cancer Res [Internet]. 2008 Jul 1 [cited 2022 Jan 19];68(13):5049–58. Available from: https://pubmed.ncbi.nlm.nih.gov/18593903/

87. Hou J, Lin L, Zhou W, Wang Z, Ding G, Dong Q, et al. Identification of miRNomes in human liver and hepatocellular carcinoma reveals miR-199a/b-3p as therapeutic target for hepatocellular carcinoma. Cancer Cell [Internet]. 2011 Feb 15 [cited 2022 Jan 19];19(2):232–43. Available from: https://pubmed.ncbi.nlm.nih.gov/21316602/

88. Wu H, Tao J, Li X, Zhang T, Zhao L, Wang Y, et al. MicroRNA-206 prevents the

pathogenesis of hepatocellular carcinoma by modulating expression of met proto-oncogene and cyclin-dependent kinase 6 in mice. Hepatology [Internet]. 2017 Dec 1 [cited 2022 Jan 19];66(6):1952–67. Available from: https://pubmed.ncbi.nlm.nih.gov/28714063/

89. Onishi M, Ochiya T, Tanaka Y. MicroRNA and liver cancer. Cancer Drug Resist [Internet]. 2020 Apr 17 [cited 2022 Jan 19];3(3):385–400. Available from: https://cdrjournal.com/article/view/3423

90. Meng F, Henson R, Wehbe-Janek H, Ghoshal K, Jacob ST, Patel T. MicroRNA-21 regulates expression of the PTEN tumor suppressor gene in human hepatocellular cancer. Gastroenterology. 2007 Aug;133(2):647–58.

91. Yu L, Zhang J, Guo X, Li Z, Zhang P. MicroRNA-224 upregulation and AKT activation synergistically predict poor prognosis in patients with hepatocellular carcinoma. Cancer Epidemiol [Internet]. 2014 [cited 2022 Jan 19];38(4):408–13. Available from: https://pubmed.ncbi.nlm.nih.gov/24923856/

92. Wu GG, Li WH, He WG, Jiang N, Zhang GX, Chen W, et al. Mir-184 Post-Transcriptionally Regulates SOX7 Expression and Promotes Cell Proliferation in Human Hepatocellular Carcinoma. PLoS One [Internet]. 2014 Feb 18 [cited 2022 Jan 19];9(2):e88796. Available from: https://journals.plos.org/plosone/article?id=10.1371/journal.pone.0088796

93. Weinstein JN, Collisson EA, Mills GB, Shaw KRM, Ozenberger BA, Ellrott K, et al. The Cancer Genome Atlas Pan-Cancer analysis project. Nat Genet 2013 4510 [Internet]. 2013 Sep 26 [cited 2022 Jan 19];45(10):1113–20. Available from: https://www.nature.com/articles/ng.2764

94. Hudson TJ, Anderson W, Aretz A, Barker AD, Bell C, Bernabé RR, et al. International network of cancer genome projects. Nat 2010 4647291 [Internet]. 2010 Apr 15 [cited 2022 Jan 19];464(7291):993–8. Available from: https://www.nature.com/articles/nature08987

95. Peng RD. Reproducible research in computational science. Science (80-). 2011 Dec 2;334(6060):1226–7.

96. Wilkinson MD, Dumontier M, Aalbersberg IjJ, Appleton G, Axton M, Baak A, et al. The FAIR Guiding Principles for scientific data management and stewardship. Sci Data 2016 31 [Internet]. 2016 Mar 15 [cited 2022 Mar 19];3(1):1–9. Available from: https://www.nature.com/articles/sdata201618

97. Vesteghem C, Brøndum RF, Sønderkær M, Sommer M, Schmitz A, Bødker JS, et al. Implementing the FAIR Data Principles in precision oncology: review of supporting initiatives. Brief Bioinform [Internet]. 2020 May 18 [cited 2022 Mar 19];21(3):936–45. Available from: https://academic.oup.com/bib/article/21/3/936/5522017

98. Containerized Bioinformatics - Bioinformatics Documentation [Internet]. [cited 2022 Mar 20]. Available from: https://www.melbournebioinformatics.org.au/tutorials/tutorials/docker/docker/

99. Bigelow SJ. Five cons of container technology [Internet]. [cited 2022 Mar 20]. Available

from: https://searchservervirtualization.techtarget.com/feature/Five-cons-of-container-technology

100. Adding custom tools to Galaxy - Galaxy Community Hub [Internet]. [cited 2022 Mar 20]. Available from: https://galaxyproject.org/admin/tools/add-tool-tutorial/

101. Kwon CH, Kim J, Ahn J. DockerBIO: Web application for efficient use of bioinformatics Docker images. PeerJ [Internet]. 2018 [cited 2022 Mar 20];2018(11). Available from: /pmc/articles/PMC6266945/

102. Köster J, Rahmann S. Snakemake—a scalable bioinformatics workflow engine. Bioinformatics [Internet]. 2012 Oct 1 [cited 2022 Feb 1];28(19):2520–2. Available from: https://academic.oup.com/bioinformatics/article/28/19/2520/290322

103. DI Tommaso P, Chatzou M, Floden EW, Barja PP, Palumbo E, Notredame C. Nextflow enables reproducible computational workflows. Nat Biotechnol 2017 354 [Internet]. 2017 Apr 11 [cited 2022 Mar 20];35(4):316–9. Available from: https://www.nature.com/articles/nbt.3820

104. Sarah Griffiths. Snakemake vs Nextflow | EPI2ME Labs Blog [Internet]. [cited 2022 Mar 20]. Available from: https://labs.epi2me.io/snakemake-vs-nextflow/

105. Panwar B, Omenn GS, Guan Y. miRmine: a database of human miRNA expression profiles. Bioinformatics. 2017 May;33(10):1554–60.

106. Anaconda Software Distribution. 2016.

107. Krueger F. Trim Galore [Internet]. 2015. Available from: https://www.bioinformatics.babraham.ac.uk/projects/trim_galore/

108. Andrews S. FastQC: A Quality Control Tool for High Throughput Sequence Data [Internet]. 2010. Available from: http://www.bioinformatics.babraham.ac.uk/projects/fastqc/

109. Wang L, Wang S, Li W. RSeQC: quality control of RNA-seq experiments. Bioinformatics. 2012 Aug;28(16):2184–5.

110. Ewels P, Magnusson M, Lundin S, Käller M. MultiQC: summarize analysis results for multiple tools and samples in a single report. Bioinformatics [Internet]. 2016 Oct 1 [cited 2022 Mar 18];32(19):3047–8. Available from: https://academic.oup.com/bioinformatics/article/32/19/3047/2196507

111. Dobin A, Davis CA, Schlesinger F, Drenkow J, Zaleski C, Jha S, et al. STAR: ultrafast universal RNA-seq aligner. Bioinformatics. 2013 Jan;29(1):15–21.

112. Bray NL, Pimentel H, Melsted P, Pachter L. Near-optimal probabilistic RNA-seq quantification. Nat Biotechnol. 2016 May;34(5):525–7.

113. Smith T, Heger A, Sudbery I. UMI-tools: modeling sequencing errors in Unique Molecular Identifiers to improve quantification accuracy. Genome Res. 2017 Mar;27(3):491–9.

114. Mullur R, Liu YY, Brent GA. Thyroid Hormone Regulation of Metabolism. Physiol Rev

[Internet]. 2014 [cited 2022 Mar 21];94(2):355. Available from: /pmc/articles/PMC4044302/

115. Soneson C, Love MI, Robinson MD. Differential analyses for RNA-seq: transcript-level estimates improve gene-level inferences. F1000Research [Internet]. 2015 Dec 30 [cited 2022 Feb 1];4:1521. Available from: https://f1000research.com/articles/4-1521

116. Love MI, Huber W, Anders S. Moderated estimation of fold change and dispersion for RNA-seq data with DESeq2. Genome Biol [Internet]. 2014 Dec 5 [cited 2022 Jan 19];15(12):1–21. Available from: https://genomebiology.biomedcentral.com/articles/10.1186/s13059-014-0550-8

117. Blighe K, Rana S LM. EnhancedVolcano: Publication-ready volcano plots with enhanced colouring and labeling. 2021;

118. Ledda-Columbano GM, Perra A, Loi R, Shinozuka H, Columbano A. Cell proliferation induced by triiodothyronine in rat liver is associated with nodule regression and reduction of hepatocellular carcinomas. Cancer Res. 2000;60(3):603–9.

119. Solt DB, Medline A, Farber E. Rapid emergence of carcinogen-induced hyperplastic lesions in a new model for the sequential analysis of liver carcinogenesis. Am J Pathol. 1977 Sep;88(3):595–618.

120. Gu J, Liu X, Li J, He Y. MicroRNA-144 inhibits cell proliferation, migration and invasion in human hepatocellular carcinoma by targeting CCNB1. Cancer Cell Int. 2019;19:15.

121. Liu AM, Poon RTP, Luk JM. MicroRNA-375 targets Hippo-signaling effector YAP in liver cancer and inhibits tumor properties. Biochem Biophys Res Commun. 2010 Apr;394(3):623–7.

122. Qian Y-Y, Li K, Liu Q-Y, Liu Z-S. Long non-coding RNA PTENP1 interacts with miR-193a-3p to suppress cell migration and invasion through the PTEN pathway in hepatocellular carcinoma. Oncotarget. 2017 Dec;8(64):107859–69.

123. Tao J, Ji J, Li X, Ding N, Wu H, Liu Y, et al. Distinct anti-oncogenic effect of various microRNAs in different mouse models of liver cancer. Oncotarget. 2015 Mar;6(9):6977–88.

124. Li H-P, Zeng X-C, Zhang B, Long J-T, Zhou B, Tan G-S, et al. miR-451 inhibits cell proliferation in human hepatocellular carcinoma through direct suppression of IKK-β. Carcinogenesis. 2013 Nov;34(11):2443–51.

125. Li P, Xiao Z, Luo J, Zhang Y, Lin L. MiR-139-5p, miR-940 and miR-193a-5p inhibit the growth of hepatocellular carcinoma by targeting SPOCK1. J Cell Mol Med. 2019 Apr;23(4):2475–88.

126. Lian J, Jing Y, Dong Q, Huan L, Chen D, Bao C, et al. miR-192, a prognostic indicator, targets the SLC39A6/SNAIL pathway to reduce tumor metastasis in human hepatocellular carcinoma. Oncotarget. 2016 Jan;7(3):2672–83.

127. Jin F, Wang Y, Li M, Zhu Y, Liang H, Wang C, et al. MiR-26 enhances chemosensitivity and promotes apoptosis of hepatocellular carcinoma cells through inhibiting autophagy.

Cell Death Dis. 2017 Jan;8(1):e2540.

128. Azumi J, Tsubota T, Sakabe T, Shiota G. miR-181a induces sorafenib resistance of hepatocellular carcinoma cells through downregulation of RASSF1 expression. Cancer Sci. 2016 Sep;107(9):1256–62.

129. Zhang Q-H, Sun H-M, Zheng R-Z, Li Y-C, Zhang Q, Cheng P, et al. Meta-analysis of microRNA-183 family expression in human cancer studies comparing cancer tissues with noncancerous tissues. Gene. 2013 Sep;527(1):26–32.

130. Xu L, Feng X, Hao X, Wang P, Zhang Y, Zheng X, et al. CircSETD3 (Hsa_circ_0000567) acts as a sponge for microRNA-421 inhibiting hepatocellular carcinoma growth. J Exp Clin Cancer Res. 2019 Feb;38(1):98.

131. Wang C, Zhu J, Zhang Z, Chen H, Ji M, Chen C, et al. Rno-miR-224-5p contributes to 2,2',4,4'-tetrabromodiphenyl ether-induced low triiodothyronine in rats by targeting deiodinases. Chemosphere. 2020 May;246:125774.

132. Macfarlane L-A, Murphy PR. MicroRNA: Biogenesis, Function and Role in Cancer. Curr Genomics. 2010 Nov;11(7):537–61.

133. Calin GA, Croce CM. MicroRNA signatures in human cancers. Nat Rev Cancer. 2006 Nov;6(11):857–66.

134. Ledda-Columbano GM, Perra A, Loi R, Shinozuka H, Columbano A. Cell proliferation induced by triiodothyronine in rat liver is associated with nodule regression and reduction of hepatocellular carcinomas. Cancer Res. 2000 Feb;60(3):603–9.

135. Wojcicka A, Piekielko-Witkowska A, Kedzierska H, Rybicka B, Poplawski P, Boguslawska J, et al. Epigenetic regulation of thyroid hormone receptor beta in renal cancer. PLoS One. 2014;9(5):e97624.

136. Menegon S, Columbano A, Giordano S. The Dual Roles of NRF2 in Cancer. Trends Mol Med. 2016 Jul;22(7):578–93.

137. Petrelli A, Perra A, Cora D, Sulas P, Menegon S, Manca C, et al. MicroRNA/gene profiling unveils early molecular changes and nuclear factor erythroid related factor 2 (NRF2) activation in a rat model recapitulating human hepatocellular carcinoma (HCC). Hepatology. 2014;59(1):228–41.

138. Zhao L, Qi Y, Xu L, Tao X, Han X, Yin L, et al. MicroRNA-140-5p aggravates doxorubicin-induced cardiotoxicity by promoting myocardial oxidative stress via targeting Nrf2 and Sirt2. Redox Biol. 2018 May;15:284–96.

139. Wang M, Wang W, Wang J, Zhang J. MiR-182 promotes glucose metabolism by upregulating hypoxia-inducible factor 1α in NSCLC cells. Biochem Biophys Res Commun. 2018 Oct;504(2):400–5.

140. Ding Z, Ericksen RE, Escande-Beillard N, Lee QY, Loh A, Denil S, et al. Metabolic pathway analyses identify proline biosynthesis pathway as a promoter of liver tumorigenesis. J Hepatol. 2020 Apr;72(4):725–35.

141. Zavattari P, Perra A, Menegon S, Kowalik MA, Petrelli A, Angioni MM, et al. Nrf2, but not β-catenin, mutation represents an early event in rat hepatocarcinogenesis. Hepatology. 2015 Sep;62(3):851–62.

142. Orrù C, Perra A, Kowalik MA, Rizzolio S, Puliga E, Cabras L, et al. Distinct Mechanisms Are Responsible for Nrf2-Keap1 Pathway Activation at Different Stages of Rat Hepatocarcinogenesis. Cancers (Basel). 2020 Aug;12(8).

143. Fornari F, Gramantieri L, Callegari E, Shankaraiah RC, Piscaglia F, Negrini M, et al. MicroRNAs in Animal Models of HCC. Cancers (Basel). 2019 Dec;11(12).

144. Ma D, Tao X, Gao F, Fan C, Wu D. miR-224 functions as an onco-miRNA in hepatocellular carcinoma cells by activating AKT signaling. Oncol Lett. 2012 Sep;4(3):483–8.

145. Vaira V, Roncalli M, Carnaghi C, Faversani A, Maggioni M, Augello C, et al. MicroRNA-425-3p predicts response to sorafenib therapy in patients with hepatocellular carcinoma. Liver Int Off J Int Assoc Study Liver. 2015 Mar;35(3):1077–86.

146. Ding J, Huang S, Wu S, Zhao Y, Liang L, Yan M, et al. Gain of miR-151 on chromosome 8q24.3 facilitates tumour cell migration and spreading through downregulating RhoGDIA. Nat Cell Biol. 2010 Apr;12(4):390–9.

147. Cao M-Q, You A-B, Zhu X-D, Zhang W, Zhang Y-Y, Zhang S-Z, et al. miR-182-5p promotes hepatocellular carcinoma progression by repressing FOXO3a. J Hematol Oncol. 2018 Jan;11(1):12.

148. Wang H, Xu J, Li D, Zhang S, Guo Z. Identification of sequence polymorphisms in the mitochondrial cytochrome c oxidase genes as risk factors for hepatocellular carcinoma. J Clin Lab Anal. 2018 Mar;32(3).

149. Miao K, Liu S-D, Huang W-X, Dong H. MiR-224 Executes a Tumor Accelerative Role during Hepatocellular Carcinoma Malignancy by Targeting Cytoplasmic Polyadenylation Element-Binding Protein 3. Pharmacology. 2020;105(7–8):477–87.

150. Du H, Zhao Y, Yin Z, Wang DW, Chen C. The role of miR-320 in glucose and lipid metabolism disorder-associated diseases. Int J Biol Sci. 2021;17(2):402–16.

151. Hyun J, Wang S, Kim J, Rao KM, Park SY, Chung I, et al. MicroRNA-378 limits activation of hepatic stellate cells and liver fibrosis by suppressing Gli3 expression. Nat Commun. 2016 Mar;7:10993.

152. Yu F, Fan X, Chen B, Dong P, Zheng J. Activation of Hepatic Stellate Cells is Inhibited by microRNA-378a-3p via Wnt10a. Cell Physiol Biochem Int J Exp Cell Physiol Biochem Pharmacol. 2016;39(6):2409–20.

153. Ayers D, Baron B, Hunter T. miRNA Influences in NRF2 Pathway Interactions within Cancer Models. J Nucleic Acids. 2015;2015:143636.

154. Li B, Li A, You Z, Xu J, Zhu S. Epigenetic silencing of CDKN1A and CDKN2B by SNHG1 promotes the cell cycle, migration and epithelial-mesenchymal transition progression of hepatocellular carcinoma. Cell Death Dis. 2020;11(10):823.

155. Liu W, Hancock CN, Fischer JW, Harman M, Phang JM. Proline biosynthesis augments tumor cell growth and aerobic glycolysis: involvement of pyridine nucleotides. Sci Rep. 2015;5(1):17206.

10. ACKNOWLEDGEMENTS

I would like to thank the following people for their generosity and help:

Professor Andrea Perra and Professor Amedeo Columbano, who gave me an opportunity to carry out my PhD and mentored me at the University of Cagliari.

Dr. Paolo Uva and Dr. Giorgio Fotia, who provided me scientific guidance and gave me the opportunity to carry out my PhD at Center for Advanced Studies, Research and Development in Sardinia (CRS4).

CRS4 HPC group for providing IT support, and for helping me out whenever I faced any issue.

Professor Diego Calvisi, who accepted and mentored me in his lab during my PhD Internship at the University of Regensburg, Germany.

Dr. Marta Anna Kowalik, who always helped me while writing the thesis, gave me constant feedback and motivation throughout the years, and also taught me all the experimental techniques. I'll always be grateful.

Dr. Matteo Masidda and Rossano Atzeni, who gave me their valuable time for teaching me everything related to Bioinformatics from scratch.

Dr. Marina Serra, who gave me absurd names, and also helped me while working in different projects, including this.

Dr. Andrea Marco Caddeo, who helped me while writing the thesis and making the plots.

My Family, who have supported and believed in me all my life. Without their support, none of this would have been possible.